Ain Shams Engineering Journal 17 (2026) 103961

Contents lists available at ScienceDirect

Ain Shams Engineering Journal

journal homepage: www.sciencedirect.com

Full length article

Stochastic resonant NLSE with cubic-quintic-septic-nonlocal nonlinearity: Soliton dynamics and noise-induced phenomena

Nafissa T. Trouba[a,b], Huiying Xu[a,*], Reham M.A. Shohib[c,*], Mohamed E.M. Alngar[d], Walaa Mahfouz[e], Xinzhong Zhu[a,f], Mahmoud Mohamed Alderiny[g]

[a] School of Computer Science and Technology, Zhejiang Normal University, Jinhua, 321004, China
[b] Zhejiang Institute of Photoelectronics, Jinhua, Zhejiang 321004, China
[c] Basic Science Department, Faculty of Economics and Business Administration, Innovation University, Sharqia, Egypt
[d] Mathematics Education Program, Faculty of Education and Arts, Sohar University, Sohar 311, Oman
[e] Deanship of Scientific Research, King Saud University, P.O. Box 2460, Riyadh 11451, Saudi Arabia
[f] College of Computer Science and Artificial Intelligence, Wenzhou University, Wenzhou 325035, China
[g] Department of Statistics and Operations Research, College of Science, King Saud University, Riyadh, 11451, Kingdom of Saudi Arabia

ARTICLE INFO

Keywords:
Stochastic NLSE
Solitons
Nonlocal effects
Itô sense
Stochastic resonance

ABSTRACT

This research examines the stochastic resonant nonlinear Schrödinger equation (NLSE) with cubic-quintic-septic nonlocal nonlinearity in the It ô framework, incorporating spatio-temporal dispersion (STD), inter-modal dispersion (IMD), resonant nonlinearities, and multiplicative white noise. Using Kudryashov's method and the P^6–model expansion approach, novel families of bright, dark, singular, Jacobi-elliptic, and periodic stochastic solitons are derived, with exact constraint conditions ensuring physical validity. Numerical simulations reveal noise-induced amplitude modulation, phase jitter, rogue-wave-like spikes, and stochastic resonance phenomena that transition periodic backgrounds into emergent soliton structures. These findings demonstrate multiplicative noise's dual role in destabilizing conventional solitons while generating resonance-enhanced coherent waveforms, filling the gap in unified models combining higher-order nonlinearities, nonlocality, and stochasticity. The numerical results were obtained using the split-step Fourier method to validate the analytical findings. The results advance soliton theory for realistic optical fibers, photonic lattices, metamaterials, and plasma systems, enabling noise-robust signal transmission and nonlinear wave control.

1. Introduction

The nonlinear Schrödinger equation (NLSE) serves as a fundamental framework in mathematical physics, characterizing the dynamics of slowly varying wave envelopes within nonlinear and dispersive media. It serves a crucial function in various physical systems, including nonlinear optics, plasma waves, Bose–Einstein condensates, and fluid dynamics [23,24]. The interplay between dispersion and nonlinear self-action in the nonlinear Schr ödinger equation results in solitons, which are localized and stable wave packets that preserve their shape while propagating. The implications of these solitons are substantial in the fields of optical communication, photonic device engineering, and nonlinear wave theory [26].

Various generalizations of the NLSE have been proposed to tackle the complexities inherent in real-world systems. Models incorporating cubic–quintic and higher-order refractive index laws have been developed to account for saturation, multi-photon absorption, and the interplay of focusing and defocusing effects [25,26]. Nonlocal nonlinearities have garnered interest due to their ability to represent long-range interactions and provide stability to waveforms, preventing collapse [11]. These extensions enhance the applicability of the NLSE to realistic optical fibers, photonic lattices, metamaterials, and plasma environments.

The fractional form of the nonlinear Schrödinger equation (NLSE) is investigated because many physical systems exhibit memory effects, anomalous dispersion, and long-range interactions that cannot be adequately described by the classical integer-order NLSE. The conformable fractional derivative offers a mathematically consistent tool to incorporate these effects while retaining useful analytical properties such as linearity and the classical chain rule

* Corresponding authors.
Email addresses: xhy@zjnu.edu.cn (H. Xu), Reham.Shohaeb@iu.edu.eg (R.M.A. Shohib).

https://doi.org/10.1016/j.asej.2025.103961
Received 9 October 2025; Received in revised form 6 December 2025; Accepted 22 December 2025
Available online 12 February 2026

A significant element frequently observed in physical systems is stochasticity. Noise sources such as thermal fluctuations, spontaneous emission, and environmental disturbances inherently influence nonlinear media. The integration of randomness into governing models is typically accomplished via stochastic extensions of the NLSE, frequently expressed in the Itô sense with multiplicative white noise [1,2,4]. Recent studies have shown that noise, often viewed as solely detrimental, can play a constructive role by inducing stochastic resonance, enhancing weak signals, and stabilizing solitons [3,6,7,16,27].

While prior stochastic NLSE models have explored cubic-quintic nonlinearities or nonlocal effects separately [1–7], the proposed model in Eq. (1) uniquely unifies cubic, quintic, and septic nonlocal nonlinearities with resonant terms, intermodal dispersion, and multiplicative noise in the Itô framework. Unlike existing studies that typically focus on lower-order nonlinearities or local responses, this work systematically incorporates higher-order refractive index saturation, nonlocality, and stochastic forcing—features that coexist in realistic optical and plasma systems. This comprehensive approach enables the derivation of new soliton families and reveals noise-driven phenomena not captured in earlier stochastic or deterministic models. Recently, considerable attention has been devoted to constructing analytical and semi-analytical solutions of nonlinear evolution equations due to their relevance in optical communication, fluid dynamics, and plasma modeling. For instance, the first-integral method has been employed to derive closed-form solutions for the Wu–Zhang system with conformable time-fractional derivatives [49], while modified mapping-type techniques have been utilized to obtain diverse exact solutions of the Davey–Stewartson model [50]. Moreover, recent studies have examined the dynamics of multidimensional optical solitons in extended conformable Kudryashov frameworks with generalized nonlinear responses [51] demonstrating the effectiveness of advanced analytical schemes. These developments provide strong motivation to further explore stochastic influences on nonlinear wave structures, as pursued in the present work.

Numerous studies have investigated stochastic soliton dynamics in various models, including the stochastic Ginzburg–Landau equation [6], the Hirota–Maccari system [7], the Konno–Oono model [8], and stochastic adaptations of the Gerdjikov–Ivanov equation [13,16]. Nevertheless, the majority of these studies are confined to lower-order nonlinearities or overlook nonlocal effects. The combined effects of cubic–quintic–septic nonlinearities, nonlocality, resonant terms, and multiplicative noise within a unified NLSE framework have yet to be systematically examined. This indicates a notable disparity, as such effects inherently coexist in realistic photonic and plasma systems.

This represents a critical research gap: no prior study unifies cubic-quintic-septic nonlocal nonlinearities, resonant terms, STD, IMD, and multiplicative Itô noise within a single NLSE framework—effects that coexist in high-power optical fibers and metamaterials [1–29,39–41].

Recent studies continue to expand the applicability and solution families of the NLSE. For instance, research has explored optical solitons in metamaterials with generalized non-local nonlinearity, highlighting novel solution behaviors in advanced media [30]. Further investigations have yielded exact solutions for the conformable fractional NLSE with Kerr and power laws, bridging fractional calculus with nonlinear optics [31]. The dynamics have also been extended to $(3+1)$-dimensional frameworks, uncovering resonant dissipative solitons that enrich the understanding of higher-dimensional wave propagation [32]. Additionally, studies on the stochastic fractional NLSE have provided insights into soliton dynamics under the combined influence of fractional derivatives and noise [33]. The analysis of cubic-quartic solitons in birefringent fibers without four-wave mixing has demonstrated the role of higher-order dispersion in sustaining stable pulses [34], while other works have focused on optical solitons with complex Ginzburg-Landau-type equations incorporating nonlinear chromatic dispersion [35]. These contributions underscore the ongoing evolution of NLSE models to capture more complex physical effects and solution structures.

The analytical approaches employed in this study, namely Kudryashov's algorithm and the P^6-model expansion method, offer distinct advantages for tackling such a complex system. Kudryashov's method is renowned for its systematic and rigorous algebraic procedure, which efficiently extracts a wide spectrum of soliton solutions—including bright, dark, and singular types—by leveraging a specially chosen auxiliary equation [36–38]. Its key strength lies in its ability to handle high-order nonlinearities without introducing unnecessary complexity. Complementarily, the P^6-model expansion method is exceptionally powerful for deriving a broader class of solutions, particularly Jacobi elliptic and periodic solutions, which can degenerate into various soliton forms under specific parameter limits. The synergy of these two methods ensures a more comprehensive and robust exploration of the model's solution space than either could achieve alone.

The incorporation of a stochastic process, specifically multiplicative noise within the Itô framework, is of profound significance as it transitions the model from an idealized, deterministic system to one that reflects the inherent randomness of real physical environments. In practical settings—be it an optical fiber subject to thermal fluctuations and spontaneous emission, a plasma with turbulent density variations, or a Bose-Einstein condensate interacting with a thermal cloud—noise is an inescapable factor. By accounting for this stochasticity, the model captures crucial phenomena such as amplitude jitter, phase diffusion, and stochastic resonance, where noise can paradoxically enhance signal transmission or stabilize wave structures. This approach reveals that noise is not merely a disruptive nuisance but a fundamental physical parameter that can dictate dynamical transitions, induce the formation of rare events like rogue waves, and ultimately govern the stability and longevity of solitons. Therefore, a stochastic analysis is indispensable for predicting the robust performance of nonlinear waves in technological applications and for achieving a more complete, physically realistic understanding of wave propagation in complex media.

Here we fill this void with Eq. (1), the first comprehensive stochastic resonant NLSE model enabling the derivation of novel bright/dark/singular/Jacobi-elliptic soliton families and revealing noise-induced rogue waves and resonance-enhanced stability unobserved in prior deterministic or lower-order stochastic analyses.

While cubic and quintic nonlinearities are well-established in models of saturable media and multiphoton processes, the inclusion of septic (seventh-order) nonlinearity is critical for accurately describing systems exhibiting extreme nonlinear optical responses. Experimentally, septic effects become significant in: ultra-high intensity laser propagation in gases and plasmas, where higher-order Kerr terms are required to model ionization and harmonic generation beyond the perturbative regime, certain photorefractive crystals and colloidal suspensions, where saturation of the refractive index change follows a higher-order polynomial law, often measurable via z-scan techniques and dense Bose-Einstein condensates with strong beyond-mean-field corrections (e.g., Lee-Huang-Yang effects), where the expansion of the equation of state includes seventh-order density terms. Including the septic term in Eq. (1) thus allows the model to capture regimes where lower-order approximations break down, particularly in experiments involving high power densities or strongly interacting quantum fluids.

This paper proposes and analyzes a stochastic resonant nonlinear Schrö dinger equation featuring cubic, quintic, and septic nonlocal nonlinearity Eq. (1). The model integrates chromatic dispersion, self-trapping dispersion (STD), intermodal dispersion (IMD), resonant nonlinearities, and multiplicative noise within the Itô framework. We utilize two complementary techniques to derive precise soliton solutions: Kudryashov's algorithms [1,2] and the P^6-model expansion approach [25–27]. These methods enable the derivation of new families of bright, dark, singular, Jacobi-elliptic, and periodic solitons.

Recent works have reported controlled shaping and deformation of bright, dark, chirped, W- and M-type solitons in nonlinear optical fibers through higher-order dispersion, birefringence, variable-coefficient effects, and nonlinear perturbations (see Refs. [42–48]). These studies

demonstrate that soliton characteristics can be significantly altered by parameter variations, external modulation, and structural changes in the governing equation. Motivated by these developments, our work considers a stochastic framework and examines how multiplicative perturbations influence soliton persistence, modulation behavior, and stability.

1.1. Main system

The dimensionless form of the stochastic resonant NLSE [1–9,15–22] is presented. It has a cubic-quintic-septic nonlocal law nonlinearity and both STD and IMD, as well as multiplicative noise in the itô sense.

$$i\Psi_t + a\Psi_{xx} + b\Psi_{xt} + \left[c_1|\Psi|^2 + c_2|\Psi|^4 + c_3|\Psi|^6 + c_4\left(|\Psi|^2\right)_{xx}\right]\Psi + \theta\left(\frac{|\Psi|_{xx}}{|\Psi|}\right)\Psi + \sigma\left(\Psi - ib\Psi_x\right)\frac{dW(t)}{dt} = i\alpha\Psi_x, \tag{1}$$

where the wave profile is represented by the complex-valued function $\Psi = \Psi(x,t)$, and the parameters $a, b, c_j, (j = 1, .., 4)$, γ, σ and α are real-valued constants with i^2 equal -1. The first term of Eq. (1) is the linear temporal evolution, the chromatic dispersion (CD) and STD terms are symbolized by a and b, respectively. The parameters c_1, c_2 and c_3 supply the cubic-quintic-septic refractive index law, whereas c_4 provides the nonlocal law. After that, θ represents the coefficient of resonant nonlinearity, and α represents the coefficient of inter-modal dispersion (IMD). At last, white noise is $dW(t)/dt$, the standard Wiener approach is denoted by $W(t)$ and σ is the noise strength coefficient. The incorporation of the stochastic term $\sigma\left(\Psi - ib\Psi_x\right)\frac{dW(t)}{dt}$ in Eq. (1) is intended to formulate a stochastic differential equation applicable across various disciplines, including physics, engineering, biology, and chemistry, which accounts for temporal noise or fluctuations. The nonlocal nonlinearity term $c_4\left(|\Psi|^2\right)_{xx}\Psi$ arises from a convolution model $n_{nl} = \int R\left(x - x'\right)\left|\Psi\left(x'\right)\right|^2 dx'$, where $R(x)$ is a symmetric response kernel (e.g., Gaussian or exponential). Expanding n_{nl} to the second order yields the differential approximation used in Eq. (1), with c_4 proportional to the second moment of $R(x)$. The spatial width σ_R of the kernel determines the degree of nonlocality:

For σ_R much larger than the soliton width, nonlinear interactions are strongly smoothed, suppressing beam collapse and stabilizing solitons against small-scale perturbations.

As $\sigma_R \to 0$, the model reduces to a local cubic-quintic-septic system, where collapse instabilities can dominate. Thus, the sign and magnitude of c_4 effectively control the stabilizing influence of nonlocality in our solutions. This mechanism is especially relevant in nematic liquid crystals, thermal optical media, and dipolar Bose–Einstein condensates, where nonlocal responses are experimentally tunable.

This article consists of the following: Section 2 delineates the first procedures. In this third section, we will resolve Eq. (1) utilizing Kudryashov's algorithm and the P^6−model expansion method. Section four will show numerical simulations. Physical interpretations are presented in Section 5. Section 6 contains the Discussion and Conclusions.

2. Preliminary steps

The objective is to uncover soliton solutions to Eq. (1). For this objective, we outline the transformation below:

$$\Psi(x,t) = F(\varsigma)\exp^{i\left[-\kappa x + \omega t + \sigma W(t) - \sigma^2 t\right]}, \varsigma = \mu x - \beta t. \tag{2}$$

In this context, κ, ω, μ and β represent non-zero constants. In this context, ω represents the wave number, μ signifies the spatial variable, β denotes the soliton's velocity, and κ indicates the soliton's frequency. The function $F(\varsigma)$ constrains the amplitude component. Substituting Eq. (2) into Eq. (1) and separating the real and imaginary components results in

$$\Re: L_1F''(\varsigma) - L_2F(\varsigma) + c_1F^3(\varsigma) + c_2F^5(\varsigma) + c_3F^7(\varsigma) + 2\mu^2c_4\left[F(\varsigma)F'^2(\varsigma) + F^2(\varsigma)F''(\varsigma)\right] = 0, \tag{3}$$

as well

$$\Im: -\left[\beta(1 - b\kappa) + \mu\left(2a\kappa - b\left(\omega - \sigma^2\right) + \alpha\right)\right]F'(\varsigma) = 0. \tag{4}$$

From Eq. (4), we get the soliton's velocity

$$\beta = -\frac{\mu\left[\alpha + 2a\kappa - b\left(\omega - \sigma^2\right)\right]}{(1 - b\kappa)}, \tag{5}$$

we balance $F^2(\varsigma)F''(\varsigma)$ with $F^7(\varsigma)$ in Eq. (3), we get:

$$2M + M + 2 = 7M \to M = \frac{1}{2}. \tag{6}$$

Here is the transformation that we employ:

$$F(\varsigma) = Z^{\frac{1}{2}}(\varsigma). \tag{7}$$

Rewrite Eq. (3) as

$$L_1\left(2Z(\varsigma)Z''(\varsigma) - Z'^2(\varsigma)\right) - 4L_2Z^2(\varsigma) + 4c_1Z^3(\varsigma) + 4c_2Z^4(\varsigma) + 4c_3Z^5(\varsigma) + 4\mu^2c_4Z^2(\varsigma)Z''(\varsigma) = 0, \tag{8}$$

where

$$L_1 = \frac{(a + \theta)(1 - b\kappa)\mu^2 + b\mu^2\left[\alpha + 2a\kappa - b\left(\omega - \sigma^2\right)\right]}{(1 - b\kappa)}, \quad L_2 = \alpha\kappa + a\kappa^2 + (1 - b\kappa)\left(\omega - \sigma^2\right). \tag{9}$$

The subsequent section will elaborate on the techniques used to address Eq. (8).

3. Novel soliton solutions

In this section, Eq. (8) is analyzed using the subsequent techniques in the following subsections:

3.1. Addendum kudryashov's algorithm

Applying the preceding technique [1,2], assume Eq. (8) has a meaningful solution:

$$Z(\varsigma) = \sum_{s=0}^{M}\sigma_s R^s(\varsigma), \theta_M \neq 0. \tag{10}$$

In addition, the $R(\varsigma)$ function fits the ODE:

$$R'^2(\varsigma) = R^2(\varsigma)\left[1 - \delta R^{2g}(\varsigma)\right]\ln^2(A), \qquad 0 < a \neq 1. \tag{11}$$

In this setting, σ_s $(s = 0, \ldots, M)$ and δ are variables, while g represents a positive integer. When we balance $Z^2(\varsigma)Z''(\varsigma)$ with $Z^5(\varsigma)$ in Eq. (8), we arrive at:

$$Z^2(\varsigma) \to 2M, Z''(\varsigma) = M + 2g \,\&\, Z^5(\varsigma) \to 5M \to 2M + M + 2g = 5M \implies M = g. \tag{12}$$

Currently let's address each of these forms:

Form.I. Given $g = 1$, $M = 1$. In place is the systematic solution:

$$Z(\varsigma) = \sigma_1 R(\varsigma) + \sigma_0, \qquad \sigma_1 \neq 0, \tag{13}$$

alongside

$$R'^2(\varsigma) = R^2(\varsigma)\left[1 - \delta R^2(\varsigma)\right]\ln^2(A), \quad 0 < a \neq 1. \tag{14}$$

Generally, Eq. (14) has a bright-singular soliton:

$$R(\varsigma)=\left[\frac{4K}{\left(4K^2+\delta\right)\cosh\left[(g\varsigma)\ln A\right]+\left(4K^2-\delta\right)\sinh\left[(g\varsigma)\ln A\right]}\right]^{\frac{1}{g}},K\neq 0. \tag{15}$$

Changing (13), (14) in (8) yields the following algebraic equations

$$\left.\begin{aligned}
&R^5(\varsigma):-4\sigma_1^3\left(2\delta\mu^2c_4\ln^2(A)-c_3\sigma_1^2\right)=0,\\
&R^4(\varsigma):-16\ln^2(A)\,\delta\mu^2c_4\sigma_0\sigma_1^2-3\ln^2(A)\,\delta L_1\sigma_1^2+20c_3\sigma_0\sigma_1^4+4c_2\sigma_1^4=0,\\
&R^3(\varsigma):-8\ln^2(A)\,\delta\mu^2c_4\sigma_0^2\sigma_1+4\ln^2(A)\,\mu^2c_4\sigma_1^3-4\ln^2(A)\,\delta L_1\sigma_0\sigma_1\\
&\quad+40c_3\sigma_0^2\sigma_1^3+16c_2\sigma_0\sigma_1^3+4c_1\sigma_1^3=0,\\
&R^2(\varsigma):8\ln^2(A)\,\mu^2c_4\sigma_0\sigma_1^2+40c_3\sigma_0^3\sigma_1^2+\ln^2(A)\,L_1\sigma_1^2+24c_2\sigma_0^2\sigma_1^2\\
&\quad+12c_1\sigma_0\sigma_1^2-4L_2\sigma_1^2=0,\\
&R(\varsigma):4\ln^2(A)\,\mu^2c_4\sigma_0^2\sigma_1+20c_3\sigma_0^4\sigma_1+2\ln^2(A)\,L_1\sigma_0\sigma_1+16c_2\sigma_0^3\sigma_1\\
&\quad+12c_1\sigma_0^2\sigma_1-8L_2\sigma_0\sigma_1=0,\\
&R^0(\varsigma):4c_3\sigma_0^5+4c_2\sigma_0^4+4c_1\sigma_0^3-4L_2\sigma_0^2=0.
\end{aligned}\right\} \tag{16}$$

Thus, Eq. (16) hold the results:

$$\left.\begin{aligned}
&c_1=\frac{\left(17L_1\ln^2(A)+20L_2\right)\mu^2c_4\ln^2(A)}{\left(5L_1\ln^2(A)+4L_2\right)},\\
&c_2=-\frac{12\left(9L_1\ln^2(A)+8L_2\right)\mu^4c_4^2\ln^4(A)}{\left(5L_1\ln^2(A)+4L_2\right)^2},\\
&c_3=\frac{32\mu^6c_4^3\ln^6(A)}{\left(5L_1\ln^2(A)+4L_2\right)^2},\sigma_0=\frac{\left(5L_1\ln^2(A)+4L_2\right)}{4\mu^2c_4\ln^2(A)},\\
&\sigma_1=\frac{\sqrt{\delta}(5L_1\ln^2(A)+4L_2)}{4\mu^2c_4\ln^2(A)}.
\end{aligned}\right\} \tag{17}$$

Given $\delta>0$. Inputting (17) and (15) into (13) completes the combo bright-singular soliton:

$$\begin{aligned}
\mathbf{\Psi}(x,t)=&\left\{\frac{(5L_1\ln^2(A)+4L_2)}{4\mu^2c_4\ln^2(A)}\right.\\
&\left.\times\left[1+\frac{4\sqrt{\delta}K}{\left(4K^2+\delta\right)\cosh(\varsigma\ln A)+\left(4K^2-\delta\right)\sinh(\varsigma\ln A)}\right]\right\}^{\frac{1}{2}}\\
&\mathrm{e}^{i\left[-\kappa x+\omega t+\sigma W(t)-\sigma^2t\right]}.
\end{aligned} \tag{18}$$

The bright soliton originates at $\delta=4K^2$.

$$\mathbf{\Psi}(x,t)=\left\{\frac{(5L_1\ln^2(A)+4L_2)}{4\mu^2c_4\ln^2(A)}\left[1+\operatorname{sech}(\varsigma\ln A)\right]\right\}^{\frac{1}{2}}\mathrm{e}^{i\left[-\kappa x+\omega t+\sigma W(t)-\sigma^2t\right]}. \tag{19}$$

Form.II. Select $g=2$ initially, followed by $M=2$. Below is what we received:

$$Z(\varsigma)=\sigma_2R^2(\varsigma)+\sigma_1R(\varsigma)+\sigma_0,\qquad \sigma_2\neq 0, \tag{20}$$

as well as

$$R'^2(\varsigma)=R^2(\varsigma)\left[1-\delta R^4(\varsigma)\right]\ln^2(A),\qquad 0<a\neq 1. \tag{21}$$

By inserting (20, 21) in (8), algebraic equations result as follows:

$$\left.\begin{aligned}
&R^{10}(\varsigma):-32\ln^2(A)\,\delta\mu^2c_4\sigma_2^3+4c_3\sigma_2^5=0,\\
&R^9(\varsigma):-76\ln^2(A)\,\delta\mu^2c_4\sigma_1\sigma_2^2+20c_3\sigma_1\sigma_2^4=0,\\
&R^8(\varsigma):-64\ln^2(A)\,\delta\mu^2c_4\sigma_0\sigma_2^2-56\ln^2(A)\,\delta\mu^2c_4\sigma_1^2\sigma_2\\
&\quad-12\ln^2(A)\,\delta L_1\sigma_2^2+20c_3\sigma_0\sigma_2^4+40c_3\sigma_1^2\sigma_2^3+4c_2\sigma_2^4=0,\\
&R^7(\varsigma):-88\ln^2(A)\,\delta\mu^2c_4\sigma_0\sigma_1\sigma_2-12\ln^2(A)\,\delta\mu^2c_4\sigma_1^3\\
&\quad-18\ln^2(A)\,\delta L_1\sigma_1\sigma_2+80c_3\sigma_0\sigma_1\sigma_2^3+40c_3\sigma_1^3\sigma_2^2+16c_2\sigma_1\sigma_2^3=0,\\
&R^6(\varsigma):-32\ln^2(A)\,\delta\mu^2c_4\sigma_0^2\sigma_2-24\ln^2(A)\,\delta\mu^2c_4\sigma_0\sigma_1^2\\
&\quad+16\ln^2(A)\,\mu^2c_4\sigma_2^3-16\ln^2(A)\,\delta L_1\sigma_0\sigma_2\\
&\quad-5\ln^2(A)\,\delta L_1\sigma_1^2+40c_3\sigma_0^2\sigma_2^3+120c_3\sigma_0\sigma_1^2\sigma_2^2+20c_3\sigma_1^4\sigma_2\\
&\quad+16c_2\sigma_0\sigma_2^3+24c_2\sigma_1^2\sigma_2^2+4c_1\sigma_2^3=0,\\
&R^5(\varsigma):-12\ln^2(A)\,\delta\mu^2c_4\sigma_0^2\sigma_1+36\ln^2(A)\,\mu^2c_4\sigma_1\sigma_2^2\\
&\quad-6\ln^2(A)\,\delta L_1\sigma_0\sigma_1+120c_3\sigma_0^2\sigma_1\sigma_2^2\\
&\quad+80c_3\sigma_0\sigma_1^3\sigma_2+4c_3\sigma_1^5+48c_2\sigma_0\sigma_1\sigma_2^2+16c_2\sigma_1^3\sigma_2+12c_1\sigma_1\sigma_2^2=0,\\
&R^4(\varsigma):32\ln^2(A)\,\mu^2c_4\sigma_0\sigma_2^2+24\ln^2(A)\,\mu^2c_4\sigma_1^2\sigma_2\\
&\quad+40c_3\sigma_0^3\sigma_2^2+120c_3\sigma_0^2\sigma_1^2\sigma_2+20c_3\sigma_0\sigma_1^4\\
&\quad+4\ln^2(A)\,L_1\sigma_2^2+24c_2\sigma_0^2\sigma_2^2+48c_2\sigma_0\sigma_1^2\sigma_2+4c_2\sigma_1^4+12c_1\sigma_0\sigma_2^2\\
&\quad+12c_1\sigma_1^2\sigma_2-4L_2\sigma_2^2=0,\\
&R^3(\varsigma):40\ln^2(A)\,\mu^2c_4\sigma_0\sigma_1\sigma_2+4\ln^2(A)\,\mu^2c_4\sigma_1^3+80c_3\sigma_0^3\sigma_1\sigma_2\\
&\quad+40c_3\sigma_0^2\sigma_1^3+6\ln^2(A)\,L_1\sigma_1\sigma_2\\
&\quad+48c_2\sigma_0^2\sigma_1\sigma_2+16c_2\sigma_0\sigma_1^3+24c_1\sigma_0\sigma_1\sigma_2+4c_1\sigma_1^3-8L_2\sigma_1\sigma_2=0,\\
&R^2(\varsigma):16\ln^2(A)\,\mu^2c_4\sigma_0^2\sigma_2+8\ln^2(A)\,\mu^2c_4\sigma_0\sigma_1^2+20c_3\sigma_0^4\sigma_2\\
&\quad+40c_3\sigma_0^3\sigma_1^2+8\ln^2(A)\,L_1\sigma_0\sigma_2\\
&\quad+\ln^2(A)\,L_1\sigma_1^2+16c_2\sigma_0^3\sigma_2+24c_2\sigma_0^2\sigma_1^2+12c_1\sigma_0^2\sigma_2+12c_1\sigma_0\sigma_1^2\\
&\quad-8L_2\sigma_0\sigma_2-4L_2\sigma_1^2=0,\\
&R(\varsigma):4\ln^2(A)\,\mu^2c_4\sigma_0^2\sigma_1+20c_3\sigma_0^4\sigma_1+2\ln^2(A)\,L_1\sigma_0\sigma_1+16c_2\sigma_0^3\sigma_1\\
&\quad+12c_1\sigma_0^2\sigma_1-8L_2\sigma_0\sigma_1=0,\\
&R^0(\varsigma):4c_3\sigma_0^5+4c_2\sigma_0^4+4c_1\sigma_0^3-4L_2\sigma_0^2=0.
\end{aligned}\right\} \tag{22}$$

Thus, Eq. (22) hold the results:

$$\left.\begin{aligned}
&c_1=\frac{4\left(17L_1\ln^2(A)+5L_2\right)\mu^2c_4\ln^2(A)}{\left(5L_1\ln^2(A)+L_2\right)},\\
&c_2=-\frac{48\left(9L_1\ln^2(A)+2L_2\right)\mu^4c_4^2\ln^4(A)}{\left(5L_1\ln^2(A)+L_2\right)^2},\\
&c_3=\frac{128\mu^6c_4^3\ln^6(A)}{\left(5L_1\ln^2(A)+L_2\right)^2},\sigma_0=\frac{\left(5L_1\ln^2(A)+L_2\right)}{4\mu^2c_4\ln^2(A)},\\
&\sigma_1=0,\sigma_2=\frac{\sqrt{\delta}(5L_1\ln^2(A)+L_2)}{4\mu^2c_4\ln^2(A)}.
\end{aligned}\right\} \tag{23}$$

Inputting (15) and (23) into (21) completes the combo bright-singular soliton:

$$\Psi(x,t)=\left\{\frac{(5L_1\ln^2(A)+L_2)}{4\mu^2c_4\ln^2(A)}\times\left[1+\frac{4\sqrt{\delta}K}{(4K^2+\delta)\cosh(2\varsigma\ln A)+(4K^2-\delta)\sinh(2\varsigma\ln A)}\right]\right\}^{\frac{1}{2}}\mathrm{e}^{i\left[-\kappa x+\omega t+\sigma W(t)-\sigma^2 t\right]}. \tag{24}$$

The bright soliton originates at $\delta=4K^2$

$$\Psi(x,t)=\left\{\frac{(5L_1\ln^2(A)+L_2)}{4\mu^2c_4\ln^2(A)}\left[1+\operatorname{sech}(2\varsigma\ln A)\right]\right\}^{\frac{1}{2}}\mathrm{e}^{i\left[-\kappa x+\omega t+\sigma W(t)-\sigma^2 t\right]}. \tag{25}$$

By varying g and M, Eq. (12) can yield numerous soliton solutions.

3.2. P^6- model expansion approach

In Eq. (8), balancing $Z^2(\varsigma)\,Z''(\varsigma)$ with $Z^5(\varsigma)$ yields the equilibrium number $M=1$. Eq. (8) has a formalized solution [25–27].

$$Z(\varsigma)=K_2P^2(\varsigma)+K_1P(\varsigma)+K_0,\quad K_2\neq 0, \tag{26}$$

and $P(\varsigma)$ satisfies:

$$P'^2(\varsigma)=\Pi_6P^6(\varsigma)+\Pi_4P^4(\varsigma)+\Pi_2P^2(\varsigma)+\Pi_0, \tag{27}$$

here K_0,K_1,K_2 and Π_l ($l=0,2,4$ & 6) are the parameters. Use the solution as a guide.

$$P(\varsigma)=\frac{\eta(\varsigma)}{\sqrt{M_1\eta^2(\varsigma)+M_2}}. \tag{28}$$

The solution to the Jacobi elliptic equation is $\eta(\varsigma)$:

$$\eta'^2(\varsigma)=\chi_0+\chi_2\,\eta^2(\varsigma)+\chi_4\eta^4(\varsigma), \tag{29}$$

χ_r (where $r=0$, 2 and 4) are parameters, and M_1 and M_2 are values given by

$$M_1=\frac{\Pi_4(\chi_2-\Pi_2)}{(\chi_2-\Pi_2)^2-2\chi_2(\chi_2-\Pi_2)+3\,\chi_0\chi_4},\qquad M_2=\frac{3\chi_0\Pi_4}{(\chi_2-\Pi_2)^2-2\chi_2(\chi_2-\Pi_2)+3\chi_0\chi_4}, \tag{30}$$

within the confines of

$$\Pi_4^2(\chi_2-\Pi_2)\left[9\chi_4\chi_0-(2\chi_2+\Pi_2)(\chi_2-\Pi_2)\right]+3\Pi_6\left[3\chi_0\chi_4-(\chi_2-\Pi_2^2)\right]^2=0,\quad \chi_2\neq\Pi_2. \tag{31}$$

Changing (26), (27) in (8) yields the following algebraic equations

$$\begin{aligned}
&P^{10}(\varsigma):\ 32c_4\mu^2K_2^3\Pi_6+4K_2^5c_3=0,\\
&P^9(\varsigma):\ 76\mu^2c_4K_1K_2^2\Pi_6+20K_1K_2^4c_3=0,\\
&P^8(\varsigma):\ 4c_2K_2^4+4c_3(K_0K_2^4+4K_1^2K_2^3+2K_2^3(2K_0K_2+3K_1^2)\\
&\quad+32\mu^2c_4(2K_0K_2+K_1^2)K_2\Pi_6\\
&\quad12L_1K_2^2\Pi_6+24\mu^2c_4K_1^2K_2\Pi_6+24\mu^2c_4K_2^3\Pi_4=0,\\
&P^7(\varsigma):\ 12\mu^2c_4(2K_0K_2+K_1^2)K_1\Pi_6+4c_3(4K_0K_1K_2^3\\
&\quad+2K_1K_2^2(2K_0K_2+3K_1^2)+4K_1K_2^2(3K_0K_2+K_1^2)\\
&\quad+16c_2K_1K_2^3+18L_1K_1K_2\Pi_6+64\mu^2c_4K_0K_1K_2\Pi_6\\
&\quad+56\mu^2c_4K_1K_2^2\Pi_4=0,\\
&P^6(\varsigma):\ 32\mu^2K_0^2K_2\Pi_6c_4+24\mu^2K_0K_1^2\Pi_6c_4+48\mu^2K_0K_2^2\Pi_4c_4\\
&\quad+40\mu^2K_1^2K_2\Pi_4c_4+16\mu^2K_2^3\Pi_2c_4\\
&\quad+40K_0^2K_2^3c_3+120K_0K_1^2K_2^2c_3+20K_1^4K_2c_3\\
&\quad+16K_0K_2^3c_2+24K_1^2K_2^2c_2+16K_0K_2L_1\Pi_6\\
&\quad+5K_1^2L_1\Pi_6+4K_2^3c_1+8K_2^2L_1\Pi_4=0,\\
&P^5(\varsigma):\ 2K_1(6\mu^2K_0^2\Pi_6c_4+32\mu^2K_0K_2\Pi_4c_4+4\mu^2K_1^2\Pi_4c_4\\
&\quad+18\mu^2K_2^2\Pi_2c_4+60K_0^2K_2^2c_3+2K_1^4c_3)\\
&\quad+2K_1(24K_0K_2^2c_2+8K_1^2K_2c_2+6K_2^2c_1+3(K_0\Pi_6+2K_2\Pi_4)L_1\\
&\quad+40K_0K_1^2K_2c_3)=0,\\
&P^4(\varsigma):\ 24\mu^2K_0^2K_2\Pi_4c_4+16\mu^2K_0K_1^2\Pi_4c_4+32\mu^2K_0K_2^2\Pi_2c_4\\
&\quad+24\mu^2K_1^2K_2\Pi_2c_4+8\mu^2K_2^3\Pi_0c_4\\
&\quad+120K_0^2K_1^2K_2c_3+20K_0K_1^4c_3+24K_0^2K_2^2c_2+48K_0K_1^2K_2c_2\\
&\quad+4K_1^4c_2+12K_0K_2^2c_1+40K_0^3K_2^2c_3\\
&\quad+12K_1^2K_2c_1+(3K_1^2\Pi_4+4K_2^2\Pi_2+12K_0K_2\Pi_4)L_1-4K_2^2L_2=0,\\
&P^3(\varsigma):\ 2K_1(4\mu^2K_0^2\Pi_4c_4+20\mu^2K_0K_2\Pi_2c_4+2\mu^2K_1^2\Pi_2c_4\\
&\quad+8\mu^2K_2^2\Pi_0c_4+40K_0^3K_2c_3+24K_0^2K_2c_2)\\
&\quad+2K_1(8K_0K_1^2c_2+12K_0K_2c_1\\
&\quad+20K_0^2K_1^2c_3-4K_2L_2)+2K_1[(2K_0+3K_2\Pi_2)\\
&L_1\Pi_4+2K_1^2c_1]=0,\\
&P^2(\varsigma):\ 16\mu^2K_0^2K_2\Pi_2c_4+8\mu^2K_0K_1^2\Pi_2c_4+16\mu^2K_0K_2^2\Pi_0c_4\\
&\quad+8\mu^2K_1^2K_2\Pi_0c_4+20K_0^4K_2c_3\\
&\quad+40K_0^3K_1^2c_3+16K_0^3K_2c_2+24K_0^2K_1^2c_2\\
&\quad+12K_0^2K_2c_1+12K_0K_1^2c_1+8K_0K_2L_1\Pi_2\\
&\quad+K_1^2L_1\Pi_2-4(2K_0K_2+K_1^2)L_2=0,\\
&P(\varsigma):\ 2K_0K_1(2\mu^2K_0\Pi_2c_4+L_1\Pi_2-4L_2)\\
&\quad+4K_0K_1(4\mu^2K_2\Pi_0c_4+5K_0^3c_3+4K_0^2c_2+3K_0c_1)=0,\\
&P^0(\varsigma):\ L_1(4K_0K_2\Pi_0-K_1^2\Pi_0)-4K_0^2L_2+4K_0^3c_1+4K_0^4c_2+4K_0^5c_3\\
&\quad+8\mu^2K_0^2K_2\Pi_0c_4=0.
\end{aligned} \tag{32}$$

Thus, Eqs. (32) hold the results:

$$K_0=0,K_1=0,K_2=\frac{(L_2-L_1\Pi_2)}{2\mu^2\Pi_0c_4},\Pi_0=\Pi_0,\Pi_2=\Pi_2,$$

$$\Pi_4=-\frac{(8\mu^2c_2c_4-3L_1c_3)(L_2-L_1\Pi_2)}{96\mu^6c_4^3\Pi_0},\Pi_6=-\frac{c_3(L_2-L_1\Pi_2)^2}{32\mu^6c_4^3\Pi_0^2},$$

$$c_1 = -\frac{96\mu^6\Pi_2 c_4^3 - 8\mu^2 L_1 c_2 c_4 + 3L_1^2 c_3}{24\mu^4 c_4^2}. \tag{33}$$

Combining (33), (26), and (28) yields the following JEF solutions:

$$F(\varsigma) = \left\{ \frac{\left(L_2 - L_1\Pi_2\right)}{2\mu^2\Pi_0 c_4} \left[\frac{\eta^2(\varsigma)}{M_1\eta^2(\varsigma) + M_2} \right] \right\}^{\frac{1}{2}}. \tag{34}$$

We will announce the updated preliminary families.**Family-I.** When $\eta(\varsigma) = \mathrm{sn}(\varsigma, m)$ or $\mathrm{cd}(\varsigma, m)$, and $0 < m < 1$, $\chi_0 = 1, \chi_2 = -\left(1 + m^2\right), \chi_4 = m^2$. Right now, we show:

$$\mathbf{\Psi}(x,t) = \left\{ \frac{48\mu^4 c_4^2}{(8\mu^2 c_2 c_4 - 3L_1 c_3)} \left[\frac{\left(-m^4 + m^2 + \Pi_2^2 - 1\right)\mathrm{sn}^2(\varsigma,m)}{(1 + m^2 + \Pi_2)\mathrm{sn}^2(\varsigma,m) - 3} \right] \right\}^{\frac{1}{2}} \mathrm{e}^{i\left[-\kappa x + \omega t + \sigma W(t) - \sigma^2 t\right]}, \tag{35}$$

or

$$\mathbf{\Psi}(x,t) = \left\{ \frac{48\mu^4 c_4^2}{(8\mu^2 c_2 c_4 - 3L_1 c_3)} \left[\frac{\left(-m^4 + m^2 + \Pi_2^2 - 1\right)\mathrm{cd}^2(\varsigma,m)}{(1 + m^2 + \Pi_2)\mathrm{cd}^2(\varsigma,m) - 3} \right] \right\}^{\frac{1}{2}} \mathrm{e}^{i\left[-\kappa x + \omega t + \sigma W(t) - \sigma^2 t\right]}, \tag{36}$$

within the bounds of this restriction

$$\Pi_4^2\left(1 + m^2 + \Pi_2\right)\left[9m^2 - \left(2 + 2m^2 - \Pi_2\right)\left(1 + m^2 + \Pi_2\right)\right] - 3\Pi_6\left[3m^2 + \left(1 + m^2 + \Pi_2^2\right)\right]^2 = 0, \quad \chi_2 \neq \Pi_2, \tag{37}$$

wheras Π_6 & Π_4 offered by (33). In addition to $m \to 1^-$, a dark soliton showed up:

$$\mathbf{\Psi}(x,t) = \left\{ \frac{48\mu^4 c_4^2}{(8\mu^2 c_2 c_4 - 3L_1 c_3)} \left[\frac{\left(\Pi_2^2 - 1\right)\tanh^2(\varsigma)}{(2 + \Pi_2)\tanh^2(\varsigma) - 3} \right] \right\}^{\frac{1}{2}} \mathrm{e}^{i\left[-\kappa x + \omega t + \sigma W(t) - \sigma^2 t\right]}, \tag{38}$$

under the constraint condition

$$\Pi_4^2\left(\Pi_2 + 2\right) - 3\Pi_6(\Pi_2 + 1)^2 = 0. \tag{39}$$

When m approaches zero, the periodic solutions become visible.

$$\mathbf{\Psi}(x,t) = \left\{ \frac{48\mu^4 c_4^2}{(8\mu^2 c_2 c_4 - 3L_1 c_3)} \left[\frac{\Pi_2^2 - 1}{(1 + \Pi_2) - 3\csc^2(\varsigma)} \right] \right\}^{\frac{1}{2}} \mathrm{e}^{i\left[-\kappa x + \omega t + \sigma W(t) - \sigma^2 t\right]}, \tag{40}$$

as well as

$$\mathbf{\Psi}(x,t) = \left\{ \frac{48\mu^4 c_4^2}{(8\mu^2 c_2 c_4 - 3L_1 c_3)} \left[\frac{\Pi_2^2 - 1}{(1 + \Pi_2) - 3\sec^2(\varsigma)} \right] \right\}^{\frac{1}{2}} \mathrm{e}^{i\left[-\kappa x + \omega t + \sigma W(t) - \sigma^2 t\right]}, \tag{41}$$

within constraints

$$\Pi_4^2\left(\Pi_2 - 2\right) - 3\Pi_6(\Pi_2 - 1)^2 = 0, \Pi_2 \neq \pm 1. \tag{42}$$

Family-II. In the event that $\chi_0 = m^2, \chi_4 = 1, \chi_2 = -\left(1 + m^2\right)$,and $\eta(\varsigma) = \mathrm{dc}(\varsigma, m)$ or $\mathrm{ns}(\varsigma, m)$, then:

$$\mathbf{\Psi}(x,t) = \left\{ \frac{48\mu^4 c_4^2}{(8\mu^2 c_2 c_4 - 3L_1 c_3)} \left[\frac{\left(-m^4 + m^2 + \Pi_2^2 - 1\right)\mathrm{dc}^2(\varsigma,m)}{(1 + m^2 + \Pi_2)\mathrm{dc}^2(\varsigma,m) - 3m^2} \right] \right\}^{\frac{1}{2}} \mathrm{e}^{i\left[-\kappa x + \omega t + \sigma W(t) - \sigma^2 t\right]}, \tag{43}$$

as well as

$$\mathbf{\Psi}(x,t) = \left\{ \frac{48\mu^4 c_4^2}{(8\mu^2 c_2 c_4 - 3L_1 c_3)} \left[\frac{\left(-m^4 + m^2 + \Pi_2^2 - 1\right)\mathrm{ns}^2(\varsigma,m)}{(1 + m^2 + \Pi_2)\mathrm{ns}^2(\varsigma,m) - 3m^2} \right] \right\}^{\frac{1}{2}} \mathrm{e}^{i\left[-\kappa x + \omega t + \sigma W(t) - \sigma^2 t\right]}. \tag{44}$$

keeping this restriction (37) in mind. To obtain the singular solitons, set m to 1^-.

$$\mathbf{\Psi}(x,t) = \left\{ \frac{48\mu^4 c_4^2}{(8\mu^2 c_2 c_4 - 3L_1 c_3)} \left[\frac{\left(\Pi_2^2 - 1\right)\coth^2(\varsigma)}{(2 + \Pi_2)\coth^2(\varsigma) - 3} \right] \right\}^{\frac{1}{2}} \mathrm{e}^{i\left[-\kappa x + \omega t + \sigma W(t) - \sigma^2 t\right]}, \tag{45}$$

with the identical restriction (39) and $\Pi_2 \neq \pm 1$.

Family-III. When $\chi_0 = -m^2, \chi_2 = 2m^2 - 1$, and $\chi_4 = 1 - m^2$, the JEF solutions are satisfied by $\eta(\varsigma) = \mathrm{nc}(\varsigma, m)$ and Eq. (1).

$$\mathbf{\Psi}(x,t) = \left\{ -\frac{48\mu^4 c_4^2}{(8\mu^2 c_2 c_4 - 3L_1 c_3)} \left[\frac{\left(-m^4 + m^2 + \Pi_2^2 - 1\right)\mathrm{nc}^2(\varsigma,m)}{(2m^2 - 1 - \Pi_2)\mathrm{nc}^2(\varsigma,m) - 3m^2} \right] \right\}^{\frac{1}{2}} \mathrm{e}^{i\left[-\kappa x + \omega t + \sigma W(t) - \sigma^2 t\right]}, \tag{46}$$

within the condition of constraint

$$\Pi_4^2\left(2m^2 - 1 - \Pi_2\right)\left[9m^2(1 - m^2) + \left(2m^2 - 1 - \Pi_2\right)\left(4m^2 - 2 + \Pi_2\right)\right] + 3\Pi_6\left[3m^2(1 - m^2) + (2m^2 - 1)^2 - \Pi_2^2\right]^2 = 0. \tag{47}$$

When $m \to 1^-$, bright solitons are maintained.

$$\mathbf{\Psi}(x,t) = \left\{ \frac{48\mu^4 c_4^2}{(8\mu^2 c_2 c_4 - 3L_1 c_3)} \left[\frac{\Pi_2^2 - 1}{3\mathrm{sech}^2(\varsigma) - (1 - \Pi_2)} \right] \right\}^{\frac{1}{2}} \mathrm{e}^{i\left[-\kappa x + \omega t + \sigma W(t) - \sigma^2 t\right]}, \tag{48}$$

under the constraint condition

$$\Pi_4^2\left(\Pi_2 + 2\right) + 3\Pi_6(\Pi_2 + 1)^2 = 0, \Pi_2 \neq \pm 1. \tag{49}$$

Family-IV. With $\chi_0 = 1, \chi_2 = 2 - m^2, \chi_4 = 1 - m^2$ and $\eta(\varsigma) = \mathrm{sc}(\varsigma, m)$ and we achieve

$$\mathbf{\Psi}(x,t) = \left\{ -\frac{48\mu^4 c_4^2}{(8\mu^2 c_2 c_4 - 3L_1 c_3)} \left[\frac{\left(-m^4 + m^2 + \Pi_2^2 - 1\right)\mathrm{sc}^2(\varsigma,m)}{(2 - m^2 - \Pi_2)\mathrm{sc}^2(\varsigma,m) + 3} \right] \right\}^{\frac{1}{2}} \mathrm{e}^{i\left[-\kappa x + \omega t + \sigma W(t) - \sigma^2 t\right]}, \tag{50}$$

under the same constraint condition

$$\Pi_4^2\left(2 - m^2 - \Pi_2\right)\left[9\left(m^2 - 1\right) + \left(2 - m^2 - \Pi_2\right)\left(4 - 2m^2 + \Pi_2\right)\right] + 3\Pi_6\left[3\left(m^2 - 1\right) + \left(2 - m^2\right)^2 - \Pi_2^2\right]^2 = 0. \tag{51}$$

For $m \to 1^-$, holding the singular soliton provides:

$$\mathbf{\Psi}(x,t) = \left\{ -\frac{48\mu^4 c_4^2}{(8\mu^2 c_2 c_4 - 3L_1 c_3)} \left[\frac{\Pi_2^2 - 1}{(1 - \Pi_2) + 3\mathrm{csch}^2(\varsigma)} \right] \right\}^{\frac{1}{2}} \mathrm{e}^{i\left[-\kappa x + \omega t + \sigma W(t) - \sigma^2 t\right]}, \tag{52}$$

provided the same condition (49). Putting m close to zero will yield the periodic solution.

$$\mathbf{\Psi}(x,t) = \left\{ -\frac{48\mu^4 c_4^2}{(8\mu^2 c_2 c_4 - 3L_1 c_3)} \left[\frac{\left(\Pi_2^2 - 1\right)\tan^2(\varsigma)}{3 + (2 - \Pi_2)\tan^2(\varsigma)} \right] \right\}^{\frac{1}{2}} \mathrm{e}^{i\left[-\kappa x + \omega t + \sigma W(t) - \sigma^2 t\right]}, \tag{53}$$

under the constraint condition

$$-\Pi_4^2\left(\Pi_2-2\right)+3\Pi_6(\Pi_2-1)^2=0,\Pi_2\neq\pm1. \tag{54}$$

Family-V. We benefit from $\eta(\varsigma)=\mathrm{cs}(\varsigma,m)$ if and only if $\chi_4=1,\chi_2=2-m^2$ and $\chi_0=1-m^2$, then, we gain

$$\boldsymbol{\Psi}(x,t)=\left\{-\frac{48\mu^4c_4^2}{(8\mu^2c_2c_4-3L_1c_3)}\left[\frac{\left(-m^4+m^2+\Pi_2^2-1\right)\mathrm{cs}^2(\varsigma,m)}{(2-m^2-\Pi_2)\mathrm{cs}^2(\varsigma,m)+3\left(1-m^2\right)}\right]\right\}^{\frac{1}{2}} \tag{55}$$

$$e^{i\left[-\kappa x+\omega t+\sigma W(t)-\sigma^2t\right]},$$

in the situation of constraint

$$\Pi_4^2\left(2-m^2-\Pi_2\right)\left[9\left(m^2-1\right)+\left(2-m^2-\Pi_2\right)\left(4-2m^2+\Pi_2\right)\right] \tag{56}$$

$$+3\Pi_6\left[3\left(m^2-1\right)+\left(2-m^2\right)^2-\Pi_2^2\right]^2=0.$$

When $m\to0^+$, the periodic solution appears as:

$$\boldsymbol{\Psi}(x,t)=\left\{-\frac{48\mu^4c_4^2}{(8\mu^2c_2c_4-3L_1c_3)}\left[\frac{\left(\Pi_2^2-1\right)\cot^2(\varsigma)}{3+\left(2-\Pi_2\right)\cot^2(\varsigma)}\right]\right\}^{\frac{1}{2}}e^{i\left[-\kappa x+\omega t+\sigma W(t)-\sigma^2t\right]}, \tag{57}$$

With the constraint condition (54) and $\Pi_2\neq\pm1$.

Family-VI. If $\chi_0=\frac{1}{4},\chi_2=\frac{1-2m^2}{2},\chi_4=\frac{1}{4}$, then $\eta(\varsigma)=\frac{\mathrm{sn}(\varsigma,m)}{1\pm\mathrm{cn}(\varsigma,m)}$, we also keep up with the JEF solutions.

$$\boldsymbol{\Psi}(x,t)=\left\{\frac{12\mu^4c_4^2}{(8\mu^2c_2c_4-3L_1c_3)}\left[\frac{\left(16m^4-16m^2-16\Pi_2^2+1\right)\mathrm{sn}^2(\varsigma,m)}{3[1\pm\mathrm{cn}(\varsigma,m)]^2+2\left(1-2m^2-2\Pi_2\right)\mathrm{sn}^2(\varsigma,m)}\right]\right\}^{\frac{1}{2}} \tag{58}$$

$$e^{i\left[-\kappa x+\omega t+\sigma W(t)-\sigma^2t\right]},$$

under the constraint condition

$$8\Pi_4^2\left(1-2m^2-2\Pi_2\right)\left[9-8\left(1-2m^2-2\Pi_2\right)\left(1-2m^2+\Pi_2\right)\right] \tag{59}$$

$$+3\Pi_6\left[3-4\left(1-2m^2\right)^2+16\Pi_2^2\right]^2=0.$$

When m approaches 1^-, maintain combination solitons.

$$\boldsymbol{\Psi}(x,t)=\left\{\frac{12\mu^4c_4^2}{(8\mu^2c_2c_4-3L_1c_3)}\left[\frac{\left(1-16\Pi_2^2\right)\tanh^2(\varsigma)}{3\left[1\pm\mathrm{sech}(\varsigma)\right]^2-2\left(1+2\Pi_2\right)\tanh^2(\varsigma)}\right]\right\}^{\frac{1}{2}} \tag{60}$$

$$e^{i\left[-\kappa x+\omega t+\sigma W(t)-\sigma^2t\right]},$$

under the constraint condition

$$-8\Pi_4^2\left(1+2\Pi_2\right)+3\Pi_6\left(4\Pi_2+1\right)^2=0,\quad\Pi_2\neq\pm\frac{1}{4}. \tag{61}$$

For obtaining periodic solutions, set m to zero:

$$\boldsymbol{\Psi}(x,t)=\left\{\frac{12\mu^4c_4^2}{(8\mu^2c_2c_4-3L_1c_3)}\left[\frac{\left(1-16\Pi_2^2\right)\tan^2(\varsigma)}{3[\sec(\varsigma)\pm1]^2+2\left(1-2\Pi_2\right)\tan^2(\varsigma)}\right]\right\}^{\frac{1}{2}} \tag{62}$$

$$e^{i\left[-\kappa x+\omega t+\sigma W(t)-\sigma^2t\right]},$$

under the constraint condition

$$-8\Pi_4^2\left(1-2\Pi_2\right)+3\Pi_6\left(4\Pi_2-1\right)^2=0,\quad\Pi_2\neq\pm\frac{1}{4}. \tag{63}$$

Family-VII. If $\chi_0=\frac{1}{4},\chi_2=\frac{1+m^2}{2},\chi_4=\frac{\left(1-m^2\right)^2}{4}$, then $\eta(\varsigma)=\frac{\mathrm{sn}(\varsigma,m)}{\mathrm{cn}(\varsigma,m)\pm\mathrm{dn}(\varsigma,m)}$ and we own the JEF solutions

$$\boldsymbol{\Psi}(x,t)=\left\{-\frac{12\mu^4c_4^2}{(8\mu^2c_2c_4-3L_1c_3)}\left[\frac{\left(m^4+14m^2-16\Pi_2^2+1\right)\mathrm{sn}^2(\varsigma,m)}{3\left[\mathrm{cn}(\varsigma,m)\pm\mathrm{dn}(\varsigma,m)\right]^2+2\left(1+m^2-2\Pi_2\right)\mathrm{sn}^2(\varsigma,m)}\right]\right\}^{\frac{1}{2}} \tag{64}$$

$$e^{i\left[-\kappa x+\omega t+\sigma W(t)-\sigma^2t\right]},$$

within a condition of constraint

$$8\Pi_4^2\left(1+m^2-2\Pi_2\right)\left[9(1-m^2)^2-8\left(1+m^2-2\Pi_2\right)\left(1+m^2+\Pi_2\right)\right] \tag{65}$$

$$+3\Pi_6\left[3(1-m^2)^2-4(1+m^2)^2+16\Pi_2^2\right]^2=0.$$

Using $m\to1^-$, yields the following singular solitons:

$$\boldsymbol{\Psi}(x,t)=\left\{-\frac{48\mu^4c_4^2}{(8\mu^2c_2c_4-3L_1c_3)}\left[\frac{\left(1-\Pi_2^2\right)\tanh^2(\varsigma)}{3\mathrm{sech}^2(\varsigma)+\left(1-\Pi_2\right)\tanh^2(\varsigma)}\right]\right\}^{\frac{1}{2}} \tag{66}$$

$$e^{i\left[-\kappa x+\omega t+\sigma W(t)-\sigma^2t\right]},$$

under the same constraint condition (39) & $\Pi_2\neq\pm1$. To maintain the same periodic solutions (62) with m near 0^+,

Family-VIII. If $\chi_0=1-m^2,\chi_2=2m^2-1,\eta(\varsigma)=\mathrm{cn}(\varsigma,m)$ & $\chi_4=-m^2$, we get

$$\boldsymbol{\Psi}(x,t)=\left\{-\frac{48\mu^4c_4^2}{(8\mu^2c_2c_4-3L_1c_3)}\left[\frac{\left(-m^4+m^2+\Pi_2^2-1\right)\mathrm{cn}^2(\varsigma,m)}{(2m^2-1-\Pi_2)\mathrm{cn}^2(\varsigma,m)+3\left(1-m^2\right)}\right]\right\}^{\frac{1}{2}} \tag{67}$$

$$e^{i\left[-\kappa x+\omega t+\sigma W(t)-\sigma^2t\right]},$$

under the constraint condition

$$-\Pi_4^2\left(2m^2-1-\Pi_2\right)\left[9m^2(1-m^2)+\left(2m^2-1-\Pi_2\right)\left(4m^2-2+\Pi_2\right)\right] \tag{68}$$

$$+3\Pi_6\left[-3m^2(1-m^2)-(2m^2-1)^2+\Pi_2^2\right]^2=0.$$

After setting $m\to0^+$, (1) maintains the same periodic solution (42).

Family-IX. If $\chi_0=-m^2\left(1-m^2\right),\eta(\varsigma)=\mathrm{ds}(\varsigma,m),\chi_2=2m^2-1$ and χ_4 equals unity, then

$$\boldsymbol{\Psi}(x,t)=\left\{-\frac{48\mu^4c_4^2}{(8\mu^2c_2c_4-3L_1c_3)}\left[\frac{\left(-m^4+m^2+\Pi_2^2-1\right)\mathrm{ds}^2(\varsigma,m)}{(2m^2-1-\Pi_2)\mathrm{ds}^2(\varsigma,m)-3m^2\left(1-m^2\right)}\right]\right\}^{\frac{1}{2}} \tag{69}$$

$$e^{i\left[-\kappa x+\omega t+\sigma W(t)-\sigma^2t\right]},$$

under the same constraint (48).

Family-X. Applying the parameters $\chi_0=\frac{1-m^2}{4},\chi_2=\frac{1+m^2}{2}$, and $\chi_4=\frac{1-m^2}{4}$, we get $\eta(\varsigma)=\mathrm{nc}(\varsigma,m)\pm\mathrm{sc}(\varsigma,m)$ or $\eta(\varsigma)=\frac{\mathrm{cn}(\varsigma,m)}{1\pm\mathrm{sn}(\varsigma,m)}$, and we maintain that

$$\boldsymbol{\Psi}(x,t)=\left\{\frac{12\mu^4c_4^2}{(8\mu^2c_2c_4-3L_1c_3)}\left[\frac{\left(m^4+14m^2-16\Pi_2^2+1\right)[\mathrm{nc}(\varsigma,m)\pm\mathrm{sc}(\varsigma,m)]^2}{2\left(1+m^2-2\Pi_2\right)[\mathrm{nc}(\varsigma,m)\pm\mathrm{sc}(\varsigma,m)]^2+3\left(1-m^2\right)}\right]\right\}^{\frac{1}{2}} \tag{70}$$

$$e^{i\left[-\kappa x+\omega t+\sigma W(t)-\sigma^2t\right]},$$

as well

$$\boldsymbol{\Psi}(x,t)=\left\{\frac{12\mu^4c_4^2}{(8\mu^2c_2c_4-3L_1c_3)}\left[\frac{\left(m^4+14m^2-16\Pi_2^2+1\right)\mathrm{cn}^2(\varsigma,m)}{2\left(1+m^2-2\Pi_2\right)\mathrm{cn}^2(\varsigma,m)+3\left(1-m^2\right)[1\pm\mathrm{sn}(\varsigma,m)]^2}\right]\right\}^{\frac{1}{2}} \tag{71}$$

$$e^{i\left[-\kappa x+\omega t+\sigma W(t)-\sigma^2t\right]},$$

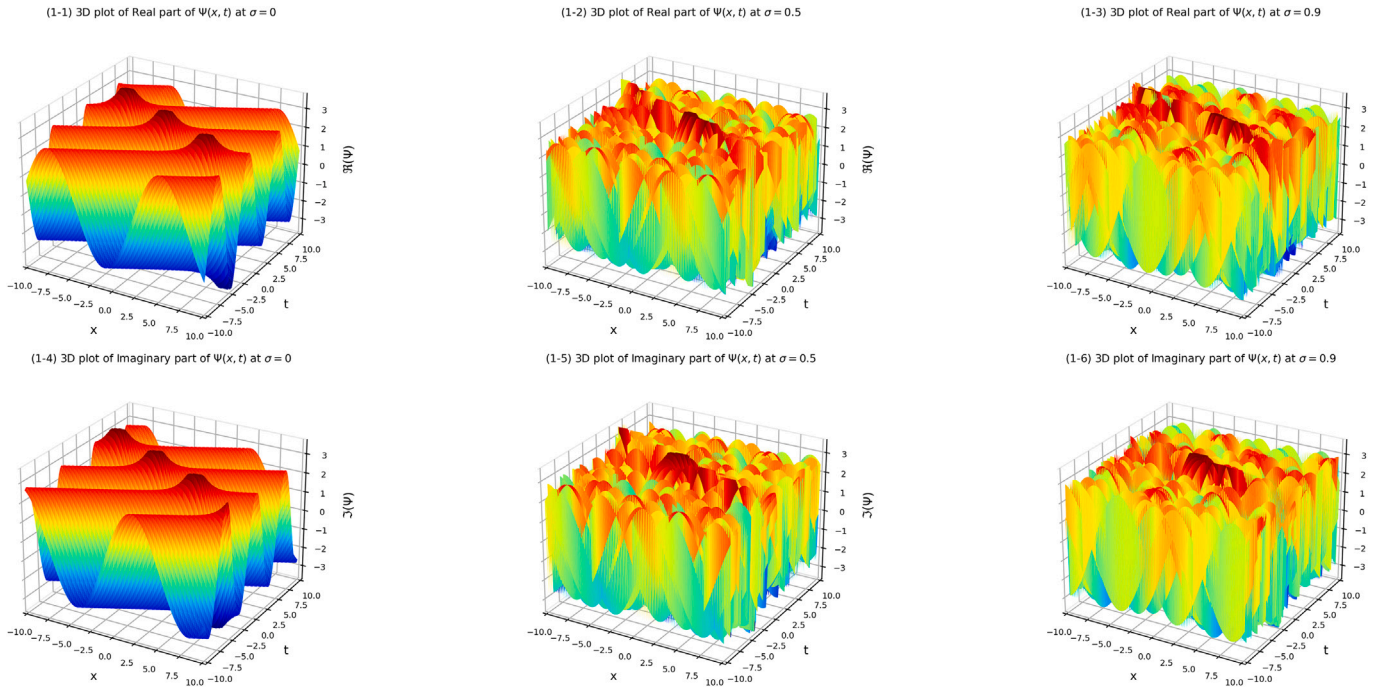

Fig. 1. Profile of a stochastic wave-type soliton corresponding to solution (19).

underneath the bounds of this limitation

$$8\Pi_4^2\left(1+m^2-2\Pi_2\right)\left[9(1-m^2)^2-8\left(1+m^2-2\Pi_2\right)\left(1+m^2+\Pi_2\right)\right] + 3\Pi_6\left[3(1-m^2)^2-4(1+m^2)^2+16\Pi_2^2\right]^2=0. \tag{72}$$

For m near 0^+ there exist periodic solutions

$$\mathbf{\Psi}(x,t)=\left\{\frac{12\mu^4c_4^2}{(8\mu^2c_2c_4-3L_1c_3)}\left[\frac{\left(1-16\Pi_2^2\right)[\sec(\varsigma)\pm\tan(\varsigma)]^2}{3+2(1-2\Pi_2)[\sec(\varsigma)\pm\tan(\varsigma)]^{22}}\right]\right\}^{\frac{1}{2}} \mathrm{e}^{i\left[-\kappa x+\omega t+\sigma W(t)-\sigma^2 t\right]}, \tag{73}$$

additionally

$$\mathbf{\Psi}(x,t)=\left\{\frac{12\mu^4c_4^2}{(8\mu^2c_2c_4-3L_1c_3)}\left[\frac{1-16\Pi_2^2}{2(1-2\Pi_2)+3[\sec(\varsigma)\pm\tan(\varsigma)]^2}\right]\right\}^{\frac{1}{2}} \mathrm{e}^{i\left[-\kappa x+\omega t+\sigma W(t)-\sigma^2 t\right]}, \tag{74}$$

that is, subject to the restriction:

$$8\Pi_4^2\left(1-2\Pi_2\right)+3\Pi_6\left(1-4\Pi_2\right)^2=0,\quad \Pi_2\neq\pm\frac{1}{4}. \tag{75}$$

4. Numerical simulations

The graphs illustrated herein represent multiple solutions to Eq. (1). The analysis of the subsequent data may elucidate specific conclusions derived from our study. The initial reference points are determined by choosing a limited subset of the defined parameter range.

Fig. 1 shows 3D graphical models of the stochastic wave-type (bright soliton) soliton corresponding to solution (19), which were made using the values $\mu=0.5,\kappa=0.5,A=2,\beta=-\left(1+\sigma^2\right)$, and the rest of the parameters $a=b=c_1=c_2=c_3=c_4=\omega=1$, as well as $W(t)=\cosh(2t)$ The graph shows the values of σ that are indicated in the legend.

Fig. 2 depicts a three-dimensional graphical representation of the stochastic (dark) wave soliton (Eq. (38)) utilizing $\kappa=-0.5,\omega=c_2=c_3=-1,\beta=-0.67\left(1+\sigma^2\right)$, and all remaining parameters set to unity. Here we take $W(t)=3-t$. Consult the legend for the σ parameter utilized in our calculations.

Fig. 3 demonstrates a 3D graphical representation of the stochastic wave singular-type soliton associated with solution (52) with $\kappa=\mu=0.5,\beta=-\left(1+\sigma^2\right)$, and the remaining parameters equal to 1, with $W(t)=\sinh\left(t^2\right)$. Please refer to the legend for the σ parameter that was employed in our calculations.

Fig. 4: Under appropriate conditions, a computer simulation of the stochastic Jacobi–elliptic wave solution (58) was executed in three dimensions with parameters $\omega=b=\mu=-1,m=1/\sqrt{3},\beta=1-0.5\sigma^2$, and the other parameters normalized to 1, with $W(t)=5t+3$. The accompanying legend illustrates the parameter value of σ employed in our computational analyses.

Fig. 5: Under appropriate conditions, a three-dimensional computer model of the stochastic wave periodic solution corresponding to Eq. (62) was executed with parameters $\mu=0.5,\kappa=-0.5,\beta=0.33\left(1-\sigma^2\right)$, with all other parameters equal to 1 and $W(t)=5t+3$. The accompanying legend illustrates the parameter value of σ employed in our computational analyses.

5. Physical interpretation

The findings yield important physical insights into soliton dynamics within the stochastic resonant nonlinear Schrödinger equation characterized by cubic, quintic, and septic nonlocal nonlinearities. Solitons manifest as stable localized waveforms in deterministic regimes, resulting from the equilibrium between dispersion and nonlinear self-focusing effects. The introduction of multiplicative noise alters this balance, resulting in amplitude modulations, phase shifts, and the emergence of new soliton families. Stochastic contributions represent realistic conditions in optical fibers, photonic systems, and plasma waves, where fluctuations from thermal noise, spontaneous emission, or environmental perturbations are inevitable.

The bright soliton solutions (Fig. 1) illustrate the stability of localized pulses amid cubic–quintic–septic nonlinearities and nonlocal effects. The higher-order terms inhibit collapse, whereas the nonlocal

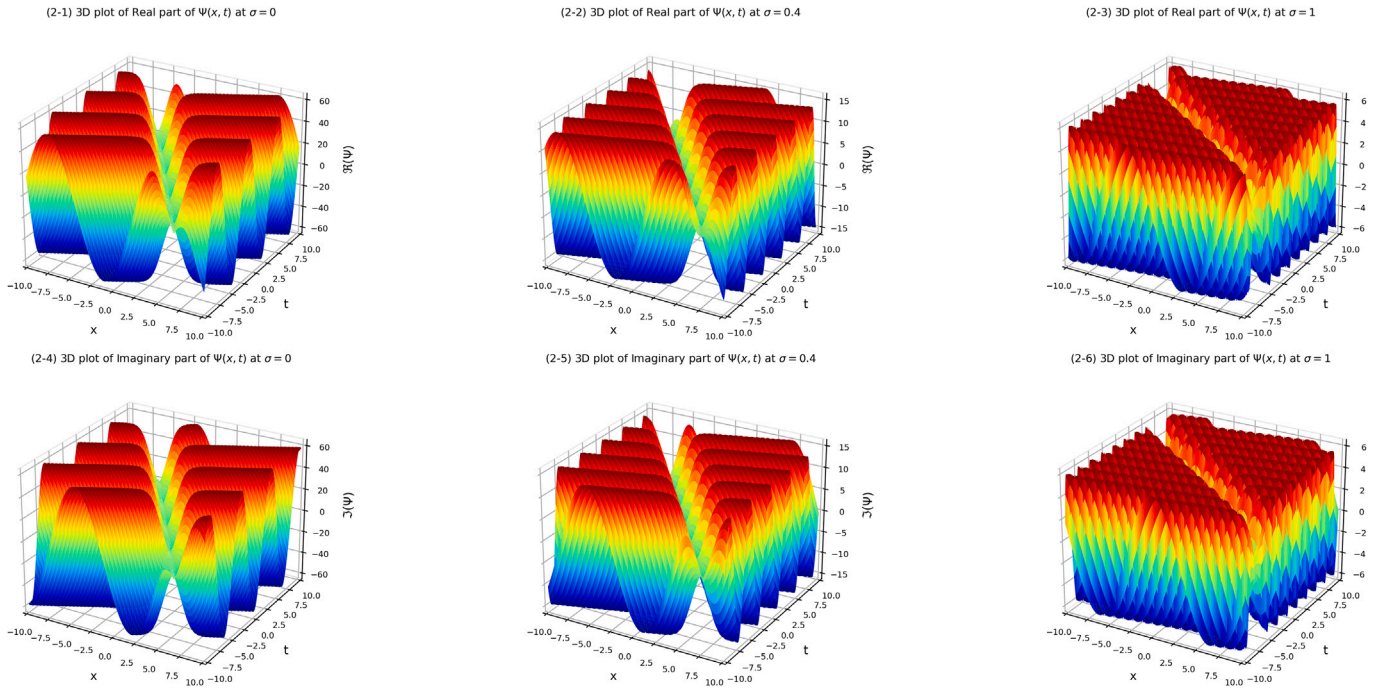

Fig. 2. Profile of a stochastic wave soliton (Eq. (38)).

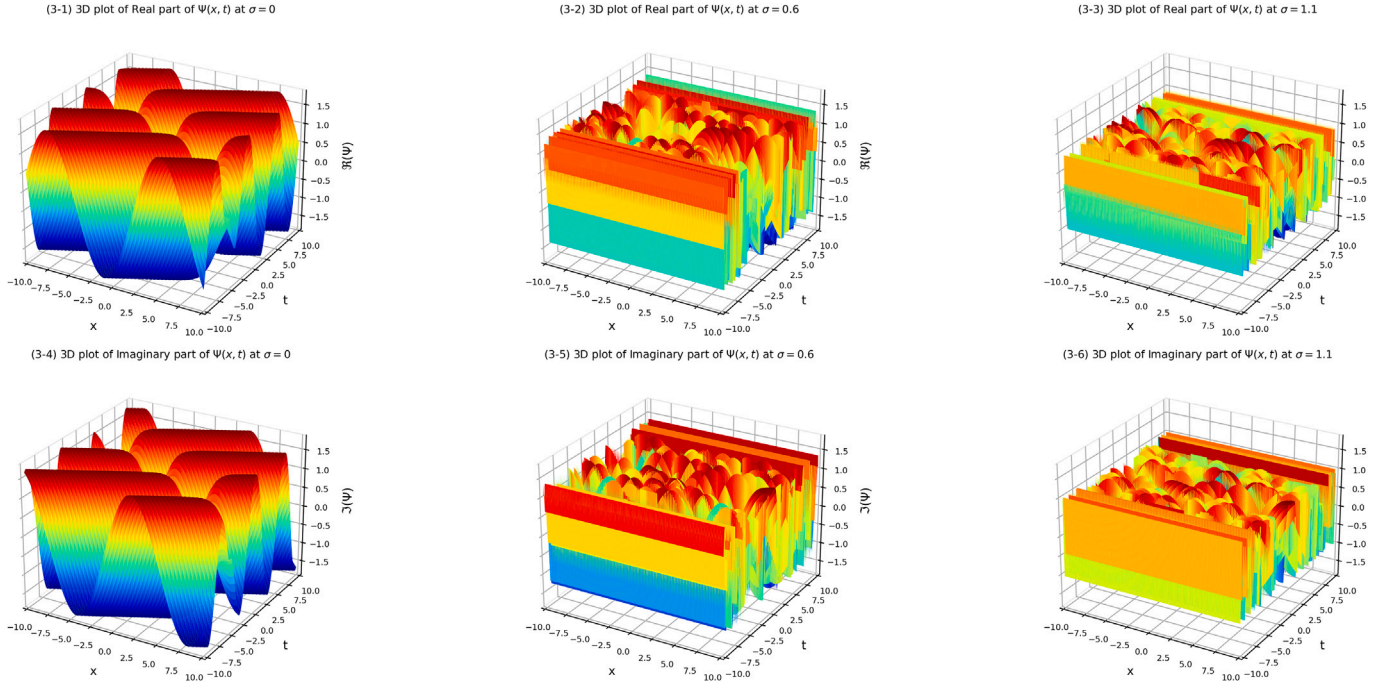

Fig. 3. Profile of a stochastic wave singular-type soliton associated with solution (52).

contribution disperses nonlinear interactions over a finite area, thereby improving stability. This denotes stable optical pulses in nonlinear fibers or photonic lattices, where randomness exists without compromising coherence.

The dark soliton solutions (Fig. 2) exhibit localized depressions within a continuous background. These occur when defocusing nonlinear contributions prevail. Stochastic perturbations cause fluctuations in soliton depth and width, suggesting that noise may destabilize or broaden the background. These dynamics are especially significant in plasma physics and defocusing optical media, where environmental noise influences nonlinear wave propagation.

The singular soliton solutions (Fig. 3) demonstrate significant localization characterized by distinct amplitude features. Stochastic perturbations enhance these structures, resulting in rogue-wave-like behavior or intensity spikes. This underscores the dual function of noise: it can disrupt smooth soliton propagation while simultaneously generating novel extreme waveforms, which may have applications in nonlinear optics and high-intensity pulse dynamics.

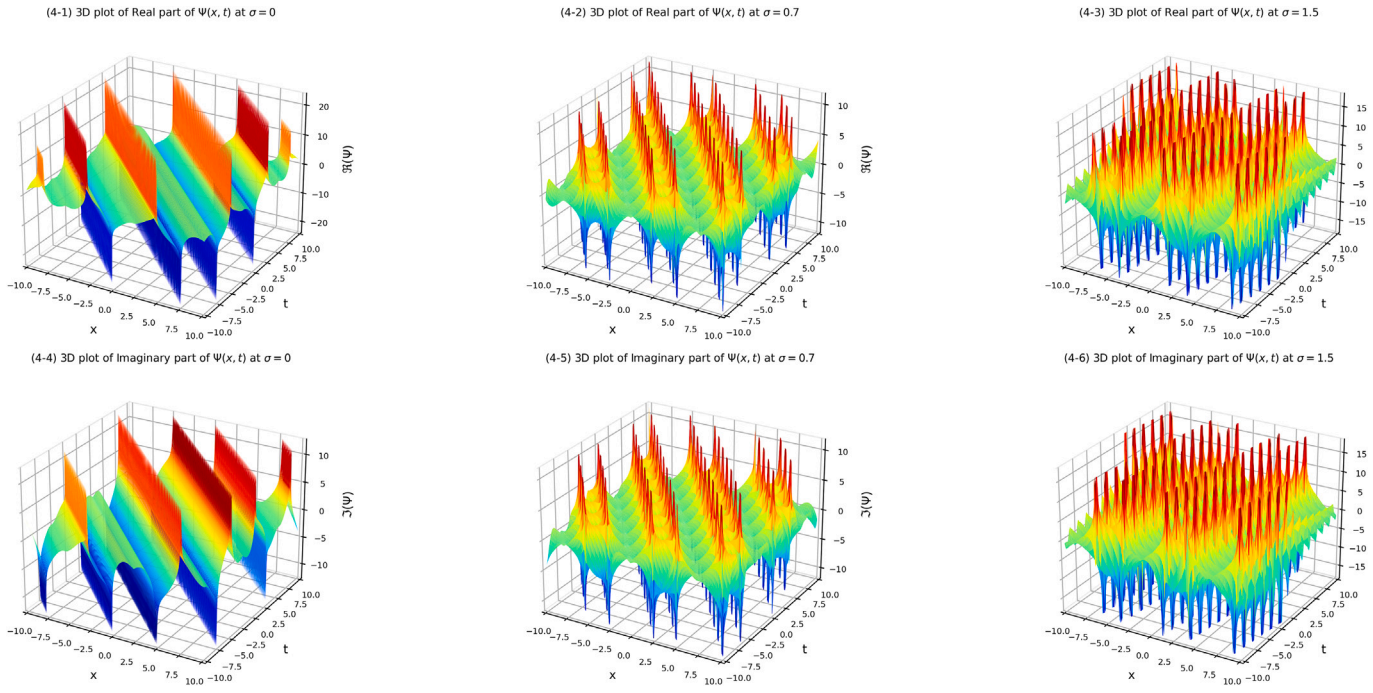

Fig. 4. Profile of a stochastic Jacobi–elliptic wave solution (58).

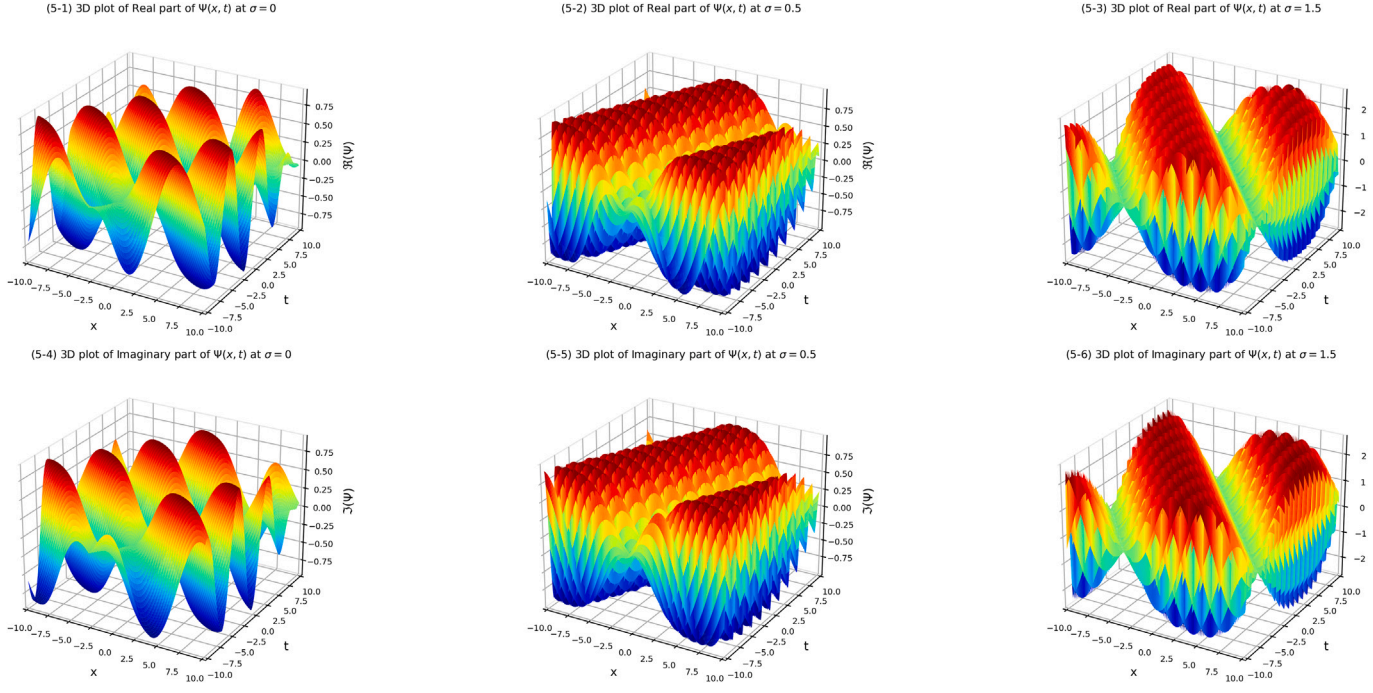

Fig. 5. Profile of the stochastic periodic-wave solution (62).

The Jacobi elliptic solutions (Fig. 4) illustrate periodic wave trains that transition smoothly between solitary and periodic states, contingent upon the elliptic modulus. Noise alters periodic backgrounds through the induction of amplitude modulation and phase jitter. These behaviors are associated with optical pulse trains in photonic lattices or nonlinear resonators, where stochastic resonance may enhance coherence or foster irregularity.

The periodic solutions illustrated in Fig. 5 exhibit soliton-like structures that recur periodically in response to stochastic forcing. These solutions connect isolated solitons with continuous periodic waves. Noise serves as a driving mechanism that facilitates transitions between solitary and periodic states, which is essential for comprehending pulse shaping and ensuring robust signal transmission in optical communication systems.

The interplay of higher-order nonlinearities, nonlocal interactions, and stochastic perturbations enhances the dynamics of soliton solutions. The data demonstrate that noise is not inherently harmful; rather, it can stabilize, modulate, or even create new soliton families via stochastic

Table 1
Dominant effects in different soliton families.

Solution (Eq.)	Dominant nonlinearity	Dominant stochastic effect	Key feature	Physical regime
(19)	Cubic + nonlocal	Moderate noise-induced phase diffusion	Stable localized pulse	Focusing media with weak noise
(38)	Quintic/septic defocusing	Noise-induced background fluctuations	Localized depression	Defocusing fibers with thermal noise
(52)	Septic + resonant term	Enhanced extreme events (rogue waves)	High-intensity spikes	High-power pulses with turbulence
(58)	Combined cubic–quintic–septic	Periodic amplitude modulation	Wave trains with elliptic periodicity	Periodic structures in photonic lattices
(62)	Nonlocal + resonant	Stochastic resonance (noise-enhanced periodicity)	Periodic recurrences	Signal amplification in noisy channels
(18)	Cubic–septic balance	Multiplicative noise stabilization	Hybrid pulse profile	Media with competing nonlinearities
(48)	Septic self-focusing	Noise-controlled collapse suppression	Collapse-arrested pulses	High-intensity beam propagation
(55)	Nonlocal defocusing	Noise-induced phase jitter	Asymmetric singular profiles	Nonlocal media with fluctuations
(60)	Higher-order dispersion	Stochastic pattern formation	Complex interference patterns	Metamaterials with disorder
(73)	Resonant + IMD	Transition enhancement (solitary ↔ periodic)	Breather-like dynamics	Active dispersion-managed systems

resonance. This research enhances theoretical comprehension and offers practical guidance for designing optical and photonic devices in noisy environments (Table 1).

Key Patterns:

(1) **Bright solitons** emerge when cubic focusing balances dispersion, with noise mainly affecting the phase.
(2) **Dark/singular solitons** require higher-order (quintic/septic) defocusing, where noise modulates the background stability.
(3) **Elliptic/periodic families** thrive under combined nonlinearities where noise induces transitions between solution types.
(5) **Stochastic resonance** is prominent in periodic solutions where noise constructively enhances signal coherence.
(6) **Nonlocal terms** generally stabilize solutions against noise-induced collapse but spread nonlinear interactions spatially.

This table reveals that specific nonlinear terms must dominate to produce each soliton type, while stochastic effects selectively amplify or modify certain features (phase, amplitude, stability). The cubic term typically drives bright solitons, septic terms enable extreme events, and nonlocal/resonant terms support structured patterns. Noise acts as a control parameter that can either disrupt or enhance these inherent nonlinear behaviors depending on its intensity and correlation with system parameters.

6. Discussion and conclusions

This paper investigated the stochastic resonant nonlinear Schrödinger equation (NLSE) that incorporates cubic-quintic-septic nonlinearities, nonlocal effects, intermodal dispersion (IMD), and multiplicative noise within the Itô framework. Kudryashov's algorithm and the P^6−model expansion method were utilized to develop a wide range of analytical soliton solutions, encompassing bright, dark, singular, Jacobi-elliptic, and periodic families. Numerical simulations validated the analytical results, demonstrated significant alignment with the theoretical framework and highlighted the influence of higher-order nonlinearities, nonlocal interactions, and stochastic forcing on soliton behavior.

The free parameters in the model—such as dispersion coefficients (a, b), nonlocality strength c_4, nonlinear coefficients c_1, c_2, c_3 the resonant term θ, the IMD coefficient α, and the noise intensity σ—directly determine the physical form of the soliton solutions. Variations in dispersion parameters modify the pulse width and propagation velocity, while adjusting the nonlinear coefficients controls the balance between focusing and defocusing effects, shaping whether the solution appears bright, dark, or singular. The nonlocality parameter regulates spatial smoothing and stabilizes or destabilizes wave profiles by spreading nonlinear interactions. Resonant and intermodal dispersion terms influence internal oscillations and phase evolution, altering the oscillatory structure of Jacobi-elliptic and periodic solutions. Finally, the stochastic noise coefficient introduces amplitude fluctuations, phase diffusion, and noise-induced modulation, determining the transition between stable, resonance-enhanced, or irregular wave behaviors. Collectively, these parameters provide precise control over the amplitude, width, localization, periodicity, and stability of the obtained soliton families.

The results obtained yield several significant insights. The incorporation of cubic–quintic–septic refractive index laws enhanced the nonlinear response of the system considerably. The cubic term governed standard self-focusing dynamics, while quintic and septic contributions mitigated potential collapse, resulting in more versatile soliton families. This underscored the need for higher-order nonlinear models to accurately represent realistic photonic and plasma systems [25,26]. The role of nonlocal nonlinearities was identified as stabilizing. Nonlocal effects, achieved through the distribution of nonlinear interactions across a finite spatial domain, reduced instabilities and facilitated the persistence of coherent soliton structures despite significant perturbations [11]. This highlighted their significance in the design of robust optical systems and metamaterials. Third, stochastic perturbations served a dual function. Multiplicative noise induced amplitude modulations, phase fluctuations, and structural transitions that could destabilize solitons.

Conversely, within suitable parameter regimes, noise could enhance soliton persistence via stochastic resonance, selectively amplifying specific modes and facilitating transitions between solitary and periodic states [1–4,6,7,27]. Contemporary research underscores the constructive role of multiplicative noise in generating bifurcation structures and stochastic resonance within NLSE frameworks featuring higher-order dispersion. Nonlocal nonlinearities further stabilize these dynamics against perturbations, enabling robust soliton propagation in realistic photonic media, while detailed analyses of stochastic NLSE characteristics confirm noise-enhanced coherence in complex systems [39–41]. The constructive role of noise highlights that randomness should not be viewed solely as harmful; instead, it could serve as a mechanism for generating or stabilizing new families of nonlinear excitations. The proposed framework is limited because it relies on reducing the stochastic model into a single ODE using a travelling-wave form, which is only valid in one-dimensional conservative settings. In higher dimensions or when gain–loss terms are added, the reduction no longer holds and the model becomes non-integrable, meaning that the same closed-form analytical solutions cannot be constructed and numerical approaches would be required instead. Despite the broad range of analytical and numerical results obtained, the present study is limited by its treatment of noise as purely multiplicative white noise within the Itô framework, which may not capture colored or experimentally correlated fluctuations. Additionally, the soliton interactions, stability under long-time evolution, and higher-dimensional effects were not explored and remain open for future investigation. These limitations suggest that extending the model to more realistic noise structures and multi-dimensional

configurations would further enhance the applicability of the framework. Lastly, the different solution sets we obtained, from localized bright and dark solitons to solitary spikes and periodic trains, show how rich soliton dynamics can be when both deterministic and stochastic factors are present. The analytical frameworks employed herein can be adapted to explore higher-dimensional stochastic NLSEs, gain–loss mechanisms, or systems characterized by saturable nonlinearities. These developments are pertinent to next-generation optical communication technology, plasma confinement research, and nonlinear wave manipulation in intricate media.

Future study may concentrate on expanding this paradigm to higher-dimensional models, examining the interactions of numerous stochastic solitons, and probing noise-induced transitions in dissipative or saturable systems. Experimental confirmation in photonic lattices, optical fibers, or Bose–Einstein condensates would serve as a logical extension, connecting theoretical predictions with realistic implementations.

This study advances the comprehension of stochastic soliton dynamics in nonlinear dispersive media and develops a thorough framework for examining the interactions of higher-order nonlinearities, nonlocality, and noise in generating complex wave patterns. The interaction of deterministic and stochastic effects expands the mathematical theory of NLSEs and offers practical applications for contemporary optical and photonic technologies. While this study derives comprehensive soliton solutions for the stochastic resonant NLSE, analytical methods are limited to specific parameter regimes and $1+1$ dimensions, with numerical simulations restricted to short-time behaviors where noise-induced instabilities may emerge. Higher-dimensional extensions, multi-soliton interactions, and long-term statistical analysis remain challenging due to SPDE complexity. Future work will explore experimental validation in photonic fibers, gain-loss models, and machine learning for stochastic soliton prediction.

CRediT authorship contribution statement

Nafissa T. Trouba: Funding acquisition, Data curation. **Huiying Xu:** Data curation, Conceptualization. **Reham M.A. Shohib:** Writing – review & editing, Writing – original draft, Software, Methodology. **Mohamed E.M. Alngar:** Writing – original draft, Software, Methodology. **Walaa Mahfouz:** Supervision, Formal analysis. **Xinzhong Zhu:** Visualization, Validation. **Mahmoud Mohamed Alderiny:** Resources, Project administration.

Use of generative-AI tools declaration

The authors declare that they have not used Artificial Intelligence (AI) tools in the creation of this article.

Declaration of competing interest

The authors declare that they have no known competing financial interests or personal relationships that could have appeared to influence the work reported in this paper.

Acknowledgements/Funding

The authors would like to thank the Ongoing Research Funding Program (ORFFT-2025–096-2), King Saud University, Riyadh, Saudi Arabia, for financial support. This work was supported by the National Natural Science Foundation of China (62376252); Key Project of Natural Science Foundation of Zhejiang Province (LZ22F030003); Zhejiang Province Leading Geese Plan (2025C02025, 2025C01056); Zhejiang Province Province-Land Synergy Program (2025SDXT004-3).

References

[1] Zayed EME, Shohib RMA, Alngar MEM, Biswas A, Yildirim Y, Dakova A, Alshehri HM, Belic MR. Optical solitons with Sasa-Sastuma model having multiplicative noise via itô calculus. Ukrain J Phys Opt 2022;23:9–14. https://doi.org/10.3116/16091833/23/1/9/2022

[2] Zayed EME, Shohib RMA, Alngar MEM. Cubic–quartic nonlinear schrödinger equation in birefringent fibers with the presence of perturbation terms. Waves in Random and Complex Media 2022;32:2445–67. https://doi.org/10.1080/17455030.2020.1854490

[3] Khan S. Stochastic perturbation of sub-pico second envelope solitons for Triki-Biswas equation with multi-photon absorption and bandpass filters. Optik. 2019;183:174–8. https://doi.org/10.1016/j.ijleo.2019.02.065

[4] Khan S. Stochastic perturbation of optical solitons having generalized anti-cubic nonlinearity with bandpass filters and multi-photon absorption. Optik. 2020;200:163405. https://doi.org/10.1016/j.ijleo.2019.163405

[5] Khan S. Stochastic perturbation of optical solitons with quadratic-cubic nonlinear refractive index. Optik. 2021;212:164706. https://doi.org/10.1016/j.ijleo.2020.164706

[6] Trouba NT, Xu H, Shohib RMA, Alngar MEM, El-Meligy M, Zhu X, Ragab AE. Stochastic soliton dynamics in the perturbed Gerdjikov-Ivanov equation with multiplicative noise via the new jacobi elliptic function expansion method. AIMS Mathematics 2025;10(11):26884–904. https://doi.org/10.3934/math.20251182

[7] Mohammed WW, Ahmad H, Hamza AE, Aly ES, El-Morshedy M, Elabbasy EM. The exact solutions of the stochastic Ginzburg-Landau equation. Results in Phys 2021;23:103988. https://doi.org/10.1016/j.rinp.2021.103988

[8] Mohammed WW, Ahmad H, Boulares H, Kheli F, El-Morshedy M. Exact solutions of HirotaMaccari system forced by multiplicative noise in the itô sense. J Low Frequency Noise Vibration Active Control 2021. https://doi.org/10.1177/14613484211028100

[9] Mohammed WW, Iqbal N, Ali A, El-Morshedy M. Exact solutions of the stochastic new coupled Konno-Oono equation. Results in Phys 2021;21:103830. https://doi.org/10.1016/j.rinp.2021.103830

[10] Mohammed WW, El-Morshedy M. The influence of multiplicative noise on the stochastic exact solutions of the Nizhnik-Novikov-Veselov system. Math Comput Simul 2021;190:192–202. https://doi.org/10.1016/j.matcom.2021.05.022

[11] Kudryashov NA. Highly dispersive optical solitons of the generalized nonlinear eighth-order schrödinger equation. Optik 2020;206:164335. https://doi.org/10.1016/j.ijleo.2020.164335

[12] Kudryashov NA. Solitary wave solutions of hierarchy with non-local nonlinearity. Appl Math Lett 2020;103:106155. https://doi.org/10.1016/j.aml.2019.106155

[13] Kudryashov NA. Highly dispersive solitary wave solutions of perturbed nonlinear schrödinger equations. Appl Math Comput 2020;371:124972. https://doi.org/10.1016/j.amc.2019.124972

[14] Kudryashov N, Lavrova S, Nifontov D. Bifurcations of phase portraits, exact solutions and conservation laws of the generalized gerdjikov–ivanov model. Mathematics 2023;11:1760. https://doi.org/10.3390/math11234760

[15] Kudryashov N, Nifontov D. Conservation laws and hamiltonians of the mathematical model with unrestricted dispersion and polynomial nonlinearity. Chaos Solitons Fract 2023;175:114076. https://doi.org/10.1016/j.chaos.2023.114076

[16] Eslami M, Mirzazadeh M, Vajargah BF, Biswas A. Optical solitons for the resonant nonlinear schrödinger's equation with time-dependent coefficients by the first integral method. Optik 2014;125:3107–16. https://doi.org/10.1016/j.ijleo.2014.01.013

[17] Eslami M, Mirzazadeh M, Biswas A. Soliton solutions of the resonant nonlinear schrödinger's equation in optical fibers with time-dependent coefficients by simplest equation approach. J Mod Opt 2013;60:1627–36. https://doi.org/10.1080/09500340.2013.850777

[18] Biswas A. Soliton solutions of the perturbed resonant nonlinear schrödinger's equation with full nonlinearity by semi-inverse variational principle. Quantum Phys Lett 2012;1:79–84.

[19] Mirzazadeh M, Eslami M, Milovic D, Biswas A. Topological solitons of resonant nonlinear schödinger's equation with dual power law nonlinearity by (G'/G) –expansion technique. Optik 2014;125:5480–9. https://doi.org/10.1016/j.ijleo.2014.03.042

[20] Triki H, Hayat T, Aldossary OM, Biswas A. Bright and dark solitons for the resonant nonlinear schrödinger's equation with time-dependent coefficients. Opt Laser Technol 2012;44:2223–31. https://doi.org/10.1016/j.optlastec.2012.01.037

[21] Triki H, Yildirim A, Hayat T, Aldossary OM, Biswas A. 1-soliton solution of the generalized resonant nonlinear dispersive schrö dinger's equation with time-dependent coefficients. Adv Sci Lett 2012;16:309–12. https://doi.org/10.1166/asl.2012.3255

[22] Zayed EME, Shohib RMA. Solitons and other solutions to the resonant nonlinear schrödinger equation with both spatio temporal and inter-modal dispersions using different techniques. Optik 2018;158:970–84. https://doi.org/10.1016/j.ijleo.2017.12.103

[23] Zhou Q, Wei C, Zhang H, Lu J, Yu H, Yaq P, Zhu Q. Exact solutions to the resonant nonlinear schrödinger equation with both spatio-temporal and inter-modal dispersions. Proc Rom Acad A 2016;17:307–13.

[24] Biswas A, Milovic D. Bright and dark solitons of the generalized nonlinear schrödinger's equation. Commun Nonlinear Sci Numer Simulat 2010;15:1173–484.

[25] Zayed EME, Al-Nowehy A-G. The Φ^6–model expansion method for solving the nonlinear conformable time-fractional schrödinger equation with fourth-order dispersion and parabolic law nonlinearity. Opt Quant Electron 2018;50:164–83. https://doi.org/10.1007/s11082-018-1426-z

[26] Zayed EME, Shohib RMA, El–Horbaty MM, Biswas A, Ekici M, Zhou Q, Alshomrani AS, Belic MR. Optical solitons in birefringent fibers with quadratic-cubic refractive index by ϕ^6– model expansion. Optik 2020;202:163620. https://doi.org/10.1016/j.ijleo.2019.163620

[27] Al Qahtani SA, Al-Rakhami MS, Shohib RMA, Alngar ME, Pathak P. Dispersive optical solitons with schrö dinger–hirota equation using the P^6- model expansion

approach. Opt Quant Electron 2023;55:701. https://doi.org/10.1007/s11082-023-04960-0
[28] Trouba NT, Xu H, Alngar MEM, Shohib RMA, Mahmoud HA, Zhu X. Soliton solutions and stability analysis of the stochastic nonlinear reaction-diffusion equation with multiplicative white noise in soliton dynamics and optical Physics. AIMS Mathematics 2025;10:1859–81. https://doi.org/10.3934/math.2025086
[29] Zayed EME, Alngar MEM, Shohib RMA. Dispersive optical solitons to stochastic resonant NLSE with both Spatio-Temporal and Inter-Modal dispersions having multiplicative white noise. Mathematics 2022;10:3197. https://doi.org/10.3390/math10173197
[30] Omar FM, Murad MAS. Analytical study of optical soliton solutions in nonlinear schrödinger model with self-steepening, self-frequency shift, and kerr nonlinearity. Mod Phys Lett B 2026;40:2550262. https://doi.org/10.1142/S0217984925502628
[31] Murad MAS, Salih MS, Arnous AH, Iqbal M. Pulse propagation of soliton solutions via the conformable fokas system in monomode optical fibers. J Opt 2025. https://doi.org/10.1007/s12596-025-02953-8
[32] Murad MAS, Mustafa MA. Formulation of soliton solutions to two-mode Sawada-Kotera equation with conformable derivative by new expanded direct mapping method. Int J Comput Math 2025:2579723. https://doi.org/10.1080/00207160.2025.2579723
[33] Omar FM, Murad MAS. Optical solitons, sensitivity analysis, chaos, and dynamics of bifurcation in the fourth-order (2+1)-dimensional nonlinear conformable schrödinger equation. Int J Comput Math 2025:2541311. https://doi.org/10.1080/00207160.2025.2541311
[34] Mustafa MA, Murad MAS. Optical soliton solutions to the generalized derivative nonlinear schrödinger equation with multiplicative white noise. J Opt 2025. https://doi.org/10.1007/s12596-025-02768-7
[35] Mustafa MA, Murad MAS. Soliton solutions to the time-fractional kudryashov equation: applications of the new direct mapping method. Mod Phys Lett B 2025;39:2550147. https://doi.org/10.1142/S0217984925501477
[36] Murad MAS, Hamasalh FK, Malik S, Arnous AH, Iqbal M. Analysis of soliton solutions to the nonlinear conformable schrö dinger equation in weakly nonlocal media using two analytic algorithms. Nonlinear Dyn 2025;113:11881–92. https://doi.org/10.1007/s11071-024-10551-9
[37] Murad MAS, Omar FM. Optical solitons, dynamics of bifurcation, and chaos in the generalized integrable (2+1)-dimensional nonlinear conformable schrödinger equations using a new kudryashov technique. J Comput Appl Math 2025;457:116298. https://doi.org/10.1016/j.cam.2024.116298
[38] Murad MAS. Optical solutions to conformable nonlinear schr ödinger equation with cubic–quintic–septimal in weakly non-local media by new kudryashov approach. Mod Phys Lett B 2025;39:2550061. https://doi.org/10.1142/S0217984925500630
[39] Akram U, Tang Z. Soliton solutions, bifurcation analysis and stochastic dynamics in nonlinear wave system. Phys Lett A 2025;553:130708. https://doi.org/10.1016/j.physleta.2025.130708
[40] Akram U, Tang Z. Bifurcation and stochastic dynamics of the Hirota-Maccari system: a study of Noise-Induced solitons. Anal.Math.Phys. 2025;15(73). https://doi.org/10.1007/s13324-025-01077-3
[41] Akram U, Alhushaybari A, Alharthi AM. Soliton-based modeling of nano-ionic currents in transmission line. Phys Fluids 2024;36:097140. https://doi.org/10.1063/5.0231980
[42] Muniyappan A, Parasuraman E, Seadawy AR, Muthuvel A. Controlled fusion and compression dynamics of w-shaped and bright solitons in birefringent optical fibers. Opt Quant Electron 2025;57(11). https://doi.org/10.1007/s11082-025-08479-4
[43] Muniyappan A, Parasuraman E, Seadawy AR, Ramkumar S. Formation of solitons with shape changing for a generalized nonlinear schr ödinger equation in an optical fiber. Opt Quant Electron 2024;56:440. https://doi.org/10.1007/s11082-023-05965-5
[44] Muniyappan A, Parasuraman E, Seadawy AR, Sudharsan JB. Chirped dark soliton propagation in optical fiber under a self phase modulation and a self-steepening effect for higher order nonlinear schr ödinger equation. Opt Quant Electron 2024;56:772. https://doi.org/10.1007/s11082-024-06358-y
[45] Muniyappan A, Sharmila M, Priya EK, Sumithra S, Biswas A, Yıldırım Y, Aphane M, Moshokoah SP, Alshehri HM. W-shaped chirp free and chirped bright, dark solitons for perturbed nonlinear schrödinger equation in nonlinear optical fibers. Proc Est Acad Sci 2023;72(2):128–44. https://doi.org/10.3176/proc.2023.2.04
[46] Muniyappan A, Manikandan K, Saparbekova A, Serikbayev N. Exploring the dynamics of dark and singular solitons in optical fibers using extended rational sinh–cosh and sine–cosine methods. Symmetry 2024;16. https://doi.org/10.3390/sym16050561
[47] Uthayakumar GS, Rajalakshmi G, Seadawy AR, Muniyappan A. Investigation of w and m shaped solitons in an optical fiber for eighth order nonlinear schrödinger (NLS) equation. Opt Quant Electron 2024;56:973. https://doi.org/10.1007/s11082-024-06730-y
[48] Manigandan M, Manikandan K, Muniyappan A, Jakeer S, Sirisubtawee S. Deformation of inhomogeneous vector optical rogue waves in the variable coefficients coupled cubic–quintic nonlinear schrödinger equations with self-steepening. Eur Phys J Plus 2024;139:405. https://doi.org/10.1140/epjp/s13360-024-05205-z
[49] Eslami M, Rezazadeh H. The first integral method for Wu-Zhang system with conformable time-fractional derivative. Calcolo 2016;53(3):475–85. https://doi.org/10.1007/s10092-015-0158-8
[50] Ahmed KK, Ahmed H, Badra NM, Mirzazadeh M, Rabie WB, Eslami M. Diverse exact solutions to Davey-Stewartson model using modified extended mapping method. Nonlinear Anal Model Control 2024;29(5):983–1002. https://doi.org/10.15388/namc.2024.29.36103
[51] Mirzazadeh M, Hashemi MS, Akbulu A, Rehman HU, Iqbal I, Eslami M. Dynamics of optical solitons in the extended (3+1)- dimensional nonlinear conformable kudryashov equation with generalized anti-cubic nonlinearity. Math Methods Appl Sci 2024;47(7):5355–75. https://doi.org/10.1002/mma.9860